Journal of Building Engineering 112 (2025) 113798

Contents lists available at ScienceDirect

Journal of Building Engineering

journal homepage: www.elsevier.com/locate/jobe

Novel ornamental lighting used to halt phototrophic colonization on architectural heritage is effective under low and high daylight illuminance conditions

Anxo Méndez [a,*], Rafael Carballeira [b], Sabela Balboa [c], Patricia Sanmartín [a]

[a] CRETUS, Gemap (GI-1243), Departamento de Edafoloxía e Química Agrícola, Facultade de Farmacia, Universidade de Santiago de Compostela, Santiago de Compostela, 15782, Spain
[b] Cavanilles Institute for Biodiversity and Evolutionary Biology, University of Valencia, 46980, Paterna, Valencia, Spain
[c] CRETUS, Departamento de Microbiología y Parasitología, CIBUS-Facultad de Biología, Universidade de Santiago de Compostela, Santiago de Compostela, 15782, Spain

ARTICLE INFO

Keywords:
Biofilm
Environmental technologies
LED luminaires
Lighting treatment
Treatment validity

ABSTRACT

Nocturnal ornamental lighting may serve as a biostatic tool to control phototrophic colonization on architectural heritage, though the influence of daylight illuminance on this effect remains unclear. This study is the first to consider the effect of the amount of daylight on responses to nocturnal lighting, by combining two levels of daylight illuminance (low, LDI, ~2050 lx and high, HDI, ~10200 lx), selected on the basis of field measurements, and three ornamental LED lighting conditions: cool white, warm white and amber + green (which has a biostatic effect on phototrophic growth) and a control (i.e. darkness). Subaerial biofilms (SABs) were generated using green algae (mainly *Chlorella vulgaris* and *Klebsormidium flaccidum*) and cyanobacteria (mainly *Synechocystis* sp.) isolated from biofilms growing on granite monuments. Changes triggered by the combination of daylight and artificial light at night were evaluated by biomass and diversity measurements, biochemical profiling, confocal microscopic examination and PAM fluorometry of mature biofilms. Cool white light enhanced biomass growth relative to the other conditions, while amber + green light halted biomass growth in both daylight scenarios. Amber + green light also decreasing the relative abundance of *Klebsormidium flaccidum* in LDI. Biofilm matrix production was reduced when illuminated with amber + green light in the LDI set-up. In the HDI set-up, all ornamental lighting conditions failed to alter the biochemical profile. However, amber + green light did reduce the R_{df} vitality index compared to other conditions. Amber + green light effectively halted biofouling under both daylight conditions, potentially mitigating its impacts and enhancing the sustainability of urban heritage management through better lighting practices.

1. Introduction

Urban structures shape urban ecosystems. Buildings block direct daylight and thus create shadows and gradients of solar irradiation on the facades and the surrounding streets (see e.g. Refs. [1–3]), with variable effects throughout the day depending on the position of the sun in the sky. Solar irradiation influences the growth of phototrophic organisms that form subaerial biofilms at the solid-air

* Corresponding author.
E-mail address: anxo.mendez.villar@usc.es (A. Méndez).

https://doi.org/10.1016/j.jobe.2025.113798
Received 24 March 2025; Received in revised form 30 July 2025; Accepted 18 August 2025
Available online 23 August 2025

interface (SABs). It thus has a direct effect on the photosynthetic capacity of the organisms [4], and it also has indirect effects by altering the temperature and moisture of the substrate on which the SABS are formed [5]. These effects determine which phototrophic organisms grow (i.e. algae or cyanobacteria) and how they are distributed on urban facades (see e.g., Ref. [6]). The aforementioned variations in solar irradiation force phototrophic organisms to manage light harvesting for photosynthesis. The organisms must achieve a balance between photochemical reactions and photoprotection from excess light to prevent oxidative damage [7], which affects their overall development (see e.g. Ref. [8]). In natural environments, organisms perform this balancing act in response to changes in correlated colour temperature (CCT, i.e. the measure of the quality, colour or wavelength of a white light) and intensity of light (see e.g. Refs. [9,10]). However, in urbanised environments, the introduction of artificial light at night (ALAN) extends the time during which phototrophic organisms must manage light exposure (see e.g. Refs. [11,12]). This particularly applies to the different CCT derived from the lighting technologies used in urban lighting (see e.g. Refs. [12,13]). For example, white LEDs and metal halide lamps emit light in the short wavelength region (i.e. around the blue region of the visible light spectra), resulting in a higher CCT, and thus have a higher relative quantum yield than high- and low-pressure sodium lamps, which have a lower CCT [12]. The artificial lighting used to illuminate heritage buildings and monuments is usually more intense than other lighting in the surrounding environment, to highlight or enhance the aesthetic value of the architecture. Longer photoperiods can promote the growth and productivity of green algae in bioreactors, in species such as *Chlorella vulgaris* [14], *Scenedesmus obliquus* (currently known as *Tetradesmus obliquus* [15]) and *Botryococcus braunii* [16]. Nevertheless, the effects of the longer photoperiods may differ in aeroterrestial biofilms, which exhibit higher tolerance to variations in light intensity and the presence of ultraviolet radiation than algal cultures (see e.g. Refs. [17, 18]).

The growth of phototrophic SABs on architectural heritage (i.e. monuments and groups of buildings with historic and artistic interest, see Ref. [19]) results in the formation of greenish coatings that stain and soil their facades. The coatings have a negative aesthetic impact and under certain circumstances may cause biodeterioration of the substrate. The generation of a coherent layer of extracellular polymeric substance (EPS) (which mainly consists of polysaccharides, proteins and eDNA) during biofilm formation provides protection to the sessile (micro)organisms within biofilms, enabling them to resist adverse conditions (e.g. high light, UV radiation, desiccation and pollutants) (see e.g. Refs. [20,21]). The extracellular matrix also serves as a refuge for other heterotrophic microorganisms such as fungi and bacteria, which can cause greater damage to heritage surfaces than phototrophs (see e.g. Refs. [22, 23]).

Algae and cyanobacteria obtain some minimal nutrients from the substrate on which they are attached to form a biofilm and/or the surrounding environment in the form of dust and soil particles ([5,24]). However, the primary source of sustenance is the light used for photosynthesis, whether daylight or artificial light. The main pigments used by phototrophs to harness light are chlorophyll *a* and *b*. The maximum absorption peaks of these pigments are usually centred in the blue and red parts of the visible light spectrum, around 428 nm and 660 nm for chlorophyll *a* [25] and 460 nm and 650 nm for chlorophyll *b* [26]. Cyanobacteria have chlorophyll *a* as the main pigment in the antenna complex, although they also have phycobilins as characteristic accessory pigments, with the blue phycocyanins absorbing in the 620–640 nm range of the spectrum with a maximum peak at 620–625 nm, and the red phycoerythrins absorbing in the 495–570 nm range of the spectrum, with a maximum peak at 540 nm (see e.g. Refs. [27,28]).

The use of artificial light to manage phototrophic colonization of heritage surfaces has already been the subject of study and implemented in underground heritage, using visible light (see e.g. Refs. [29,30]) and even UV radiation (see e.g. Ref. [31]). With the absence of natural sunlight in underground heritage sites [30], demonstrated that the photosynthetic activity was higher in cyanobacterial biofilms located closer to artificial light sources. These authors also reported a reduction in the emission spectra of the biofilm caused by the absorption of light due to the intrinsic characteristics of the phototrophic community. This observation suggests that the photosynthetic apparatus of these biofilms acclimates in response to light quality and intensity, as determined by the spectral composition and proximity to the artificial light source (fluorescent lamps with emission peaks at 540 nm and 575–632 nm).

As it is not possible to modify the exposure of outdoor building/monument facades to daylight, ornamental lighting can be used in an alternative approach to managing or even reducing phototrophic colonization on architectural heritage. The advent of LED technology has caused a notable shift in the range of light spectra available for nocturnal illumination, enabling more precise control of the wavelengths emitted [32]. This presents an opportunity to illuminate facades at the ranges within which the absorption of photosynthetic pigments is low, such as the amber and green region of the visible light (PAR: Photosynthetically Active Radiation) spectrum [33]. This could potentially control the development of phototrophic organisms and their subsequent impact by using existing lighting infrastructure. Thus, ornamental illumination could ultimately be used in a multifunctional approach to maintaining the ornamental illumination of architectural heritage while enhancing protection against SABs. It was within this context that the CromaLux project (http://cromalux.santiagodecompostela.gal/en) arose. The project focuses on how to reduce SABs growth on architectural heritage by using suitable white-like light and has led to the development of a novel LED lighting system with a biostatic effect (halting biological colonization, mainly caused by algae and cyanobacteria) based on the combination of amber and green LED lights. However, it is not clear whether application of this novel LED lighting at night is affected by different sunlight scenarios during the daytime, i.e. low and high daylight illuminance (i.e. total luminous flux incident on a surface, per unit area). It is also not yet known whether the intensity of daylight affects the SABs formed under exposure to ornamental light. The present study investigated the effects of high daylight illuminance (hereinafter, HDI) and low daylight illuminance (hereinafter, LDI) in combination with four night-time ornamental light regimes, i.e. cool white LED (CCT, 4300K), warm white light LED (CCT, 2580K) and amber + green LED (CCT, 3000K, potentially with a biostatic effect) and a control without light (i.e. darkness) on laboratory-grown phototrophic multi-species SABs. The HDI and LDI levels were based on field measurements made in facades with different orientations in the urban fabric. Growth and diversity, biochemical profiling (pigment production, exopolysaccharides and levels of ATP), confocal microscopy and pulse-amplitude modulated (PAM) fluorometry of the target SABs were used to evaluate the efficiency and effects of the new

ornamental lighting (amber + green) relative to other ornamental lighting and in relation to high and low levels of daylight. If the biostatic capacity is confirmed under varying daylight irradiance conditions, ornamental nocturnal lighting could serve as an effective tool for mitigating phototrophic colonization across a broader range of urban heritage structures. Thus, the end-goal is to reduce the frequency of cleaning interventions with more efficient ornamental illumination practices and thereby enhancing the sustainability of urban architectural heritage management.

2. Material and methods

2.1. Experimental lighting set-up

The lighting set-up consisted of a custom-built cabinet, divided into four compartments. An artificial photoperiod was established in each compartment (Fig. 1a), consisting of 13 h of LED simulating daylight (SUN@HOME, Spot PAR16 40 GU10 TW, Ledvance, Germany) with a colour temperature of 5500K, followed by 6 h of three different nocturnal ornamental LED lights (cool white, warm white and amber + green, the latter with potentially biostatic effect) and a control with no nocturnal light (i.e. darkness). The photoperiod ended with 5 h of darkness for all different light regimes. The ornamental lighting consisted of illuminance of 20 lux, supplied by a radiometer (DHD 2302.0, HERTER). This is the minimum level recommended for highlighting facades and is in keeping with the principles of energy conservation and reduction of light pollution (see e.g. Ref. [34]). Lux, lx (lumen per m^2) was chosen as the unit of luminous illuminance because it is the unit used in the regulations for Spanish ornamental and urban lighting (see Ref. [35]), regardless of light spectrum emitted by the light source used. Three ornamental lights were tested: cool white (4300K, 1.84 μmol s^{-1} m^{-2}, A5 GU10 9W, Aigostar, Spain), warm white (2580K, 1.13 μmol s^{-1} m^{-2}, cod. 671992, Televés, Spain) and a combination of monochromatic amber plus green LED lights (3000K, 0.89 μmol s^{-1} m^{-2}, cod. 671990-1, Televés, Spain). Both white lights emit the full range of the visible light spectrum (≈380 nm–700 nm), with the cool white generating a bluish tone due to the main peak being at 457 nm. The cool white LED was shaded with a slightly yellowish, heat-resistant paper film to dim the light to an illuminance of 20 lx, resulting in a change in the correlated colour temperature (CCT) from 6400K (as specified by the manufacturer) to 4300K, which is more similar to outdoor cool white light sources such as metal halide lamps (see Ref. [36]). The warm white LEDs are characterised by a reduction in the blue region (with a secondary, less intense peak at 450 nm), resulting in a yellowish tone with the main peak around 600 nm. The amber + green LED emits a bimodal spectrum with two peaks, one at 528 nm (green) and a main peak at 593 nm (amber), with no emission at wavelengths in the blue and red parts of the spectrum. The complete photoperiod is depicted in Fig. 1a, and the light spectra of daylight and ornamental LED lights are shown in Fig. 1b.

The experiment was conducted twice under identical experimental conditions, except for the daylight illuminance. Two daylight

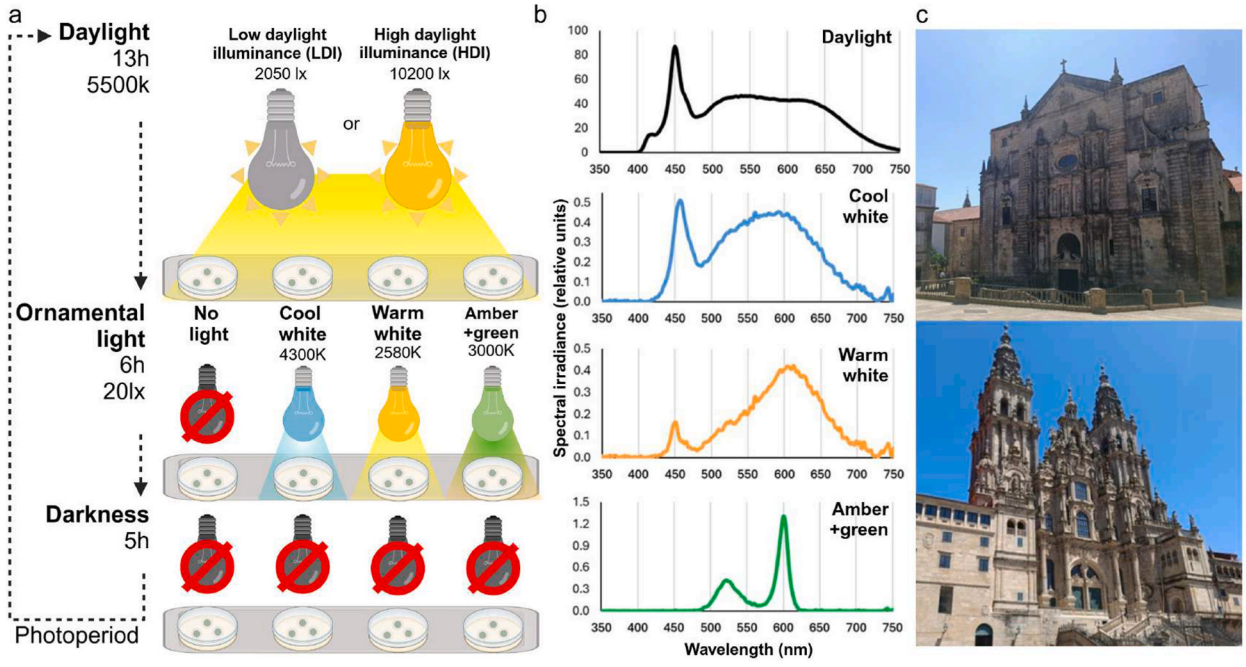

Fig. 1. a) Diagram illustrating the experimental design, including the characteristics of the photoperiod used to culture subaerial biofilms (SABs); b) Emission spectra of the lights used. The daylight irradiance level corresponds to high daylight illuminance (HDI). c) Examples of some of the surveyed facades in the historical centre of Santiago de Compostela, which are exposed during daytime to low levels of solar illuminance (upper image, Church of the Convent of San Martiño Pinario, east-(slightly north)facing) and high levels of solar illuminance (lower image, Cathedral of Santiago de Compostela main entrance, west-(slightly south)facing) (images provided by Anxo Méndez).

regimes were selected: one of low solar illuminance (LDI) and the other of high solar illuminance (HDI). Two surveys (one on a cloudy day and one in a sunny day) were conducted in the spring of 2022, at midday, on various facades of the architectural heritage of the historical centre of Santiago de Compostela (Fig. 1c). Eight granite heritage buildings were selected according to their orientation, position and surrounding architecture: three being subjected to direct insolation and five subjected to indirect insolation throughout the day. Examples of two the surveyed facades are shown in Fig. 1c. The direct insolation ranged at midday between around 2000 to 2500 lux in the cloudy day and 40,000 to 60,000 lux in the sunny day, while the indirect insolation ranged between around 1000 to 3,00 lux in the cloudy day and 2000 and 6000 lux in the sunny day. The seasonal average daily insolation in the city, as reported by the Galician meteorological service (https://www.meteogalicia.gal/), was used to assess whether the cumulative solar illuminance applied during the 13-h daylight period was consistent with the daily insolation in spring. Considering the aforementioned factors, an illuminance level of approximately 2050 lux (50.07 μmol s^{-1} m^{-2}) was determined for the LDI (simulating an indirect facade or a cloudy day) and 10200 lux (252.59 μmol s^{-1} m^{-2}) for the HDI (simulating a direct facade on a sunny day).

2.2. Biofilm culture and SAB formation

Subaerial biofilms (SABs) were prepared following a previously described procedure [37]. The SABs were generated using Bold's Basal Medium (BBM) liquid cultures derived from natural phototrophic biofilms growing on architectural heritage built in granite of the historical centre of Santiago de Compostela (UNESCO World Heritage City since 1985, north-western Spain), mainly composed of green algae but also including cyanobacteria. The species grown in the broth culture were examined under light microscopy, with a Nikon Eclipse E600 equipped with an E-Plan 40 × objective (N.A. 0.65) and differential interference contrast (Nomarski) optics. Taxonomic determinations were based on the morphometry and reproduction of the species isolated from the culture. The main taxonomic references used for the identification of green algae were [38–41] for cyanobacteria.

Aliquots of a suspension of exponentially growing cells (50 μL, equivalent to depositing a dry weight biomass of 6.85 x10^{-2} μg for the experiment under the LDI conditions and 7.60 x10^{-2} μg for the experiment under the HDI conditions) were used to inoculate the shiny side of each sterile polycarbonate membrane disc (Nuclepore™ track-etch membrane filtration products, diameter 2.5 cm, area 4.9 cm^2, pore diameter 0.2 μm, Whatman™). The membrane discs were sterilized by exposure to UV-C light (Philips TUV F17T) for 1 h on each of the two sides (shiny and matt). Three membranes were placed in each of four BBM agar plates. One plate was then placed in each compartment in the cabinet, for exposure to the ornamental light regimes tested (cool white, warm white, amber + green, and no light), under LDI and then HDI conditions (Fig. 1). The membranes were transferred, with the aid of plastic forceps, to fresh agar plates twice a week, to ensure full nutrient availability. The subaerial biofilms (SABs) were cultured for 37 days until they reached maturity. Twelve membranes (three per ornamental light regime) were then selected at random for analysis by confocal microscopy. The remaining membranes were subjected to PAM fluorometry tests and biomass determination. Of these, three groups of three membranes per ornamental light regime were randomly selected for pigment quantification (chlorophylls *a* and *b*), extracellular polymeric substance (EPS) matrix analysis and diversity study.

2.3. Biomass and diversity

The mature biofilms (37 days old) on membrane discs were weighed on a precision laboratory balance (Denver Instruments). Whole colonies were then removed from the membrane discs by gentle scraping with a sterile loop and transferred to a tube containing 1.5 mL of Phosphate-Buffered Saline (PBS). Colonies used for EPS analysis were suspended in 2 mL of 2 % ethylenediaminetetraacetic acid (EDTA). Homogeneous suspensions were used for subsequent determination of pigment content, EPS matrix and analysis of species diversity. The biofilm was removed from the membrane discs, which were then re-weighed on the same balance. The wet weight biomass of the biofilm was determined as the difference between the weight of the discs before and after the biofilm was removed.

Membranes intended for species diversity analysis were used to quantify the cell concentration (n° cell mg^{-1} SAB) in an Utermöhl sedimentation chamber [42], with at least 1000 cells counted across 100 fields at 40 × magnification. Changes in specific diversity were examined and determined by the same taxonomic techniques and equipment already described (see Section 2.2).

2.4. Biochemical profile

Homogeneous suspensions of biofilm in PBS were resuspended in 2 mL of dimethylsulfoxide (DMSO, Sigma Aldrich, Italy), heated to 65 °C for 1 h [43] and centrifuged for 10 min at 7000g. The supernatant was then collected from each sample and used to determine the chlorophyll (a and b) contents by spectrophotometric measurements (UV/VIS Spectrometer T8DCS, Persee, Germany). The values were calculated using the equations proposed by Ref. [44].

The main extracellular polymeric substances (EPS) (i.e. exopolysaccharides and extracellular proteins) were extracted using a modified version of the method described by Ref. [45] with the modifications described by Ref. [46]. The extracellular matrix was separated from the cells by placing the biofilm samples in 2 % EDTA and sonicating them at 40Hz in a water bath for 10 min. The samples were then incubated for 3 h at 4 °C and centrifuged at 300 rpm for 20 min. The supernatant was centrifuged again, at 5000 rpm for 20 min at 4 °C, and then filtered through 0.22 μm filter paper. The filtrate was placed in ethanol and left overnight at −20 °C to precipitate. The pellet obtained after centrifugation of the precipitate at 13000 rpm for 30 min was then resuspended in M9 minimal medium. The exopolysaccharide fraction of the supernatant was quantified spectrophotometrically in microplates at 490 nm in a Multiskan SkyHigh spectrophometer (Thermo Sicentific) and analysed with Skanlt Software, by the phenol-sulphuric acid method [47]

with D (+)-glucose (Panreac) as standard. The protein content was measured using the Bradford assay [48].

The ATP content was determined in aliquots (0.5 mL) of the biofilm samples in PBS and ATP, by using a luminometry-based cell viability kit (Cell Viability Kit AB, BioTherma, Sweden) and following the luciferase-based protocol for tube luminometers (Junior LB 9509, Berthold Technologies, Germany). Luminescence units (RLU) were converted to ATP concentration (pmol) according to the manufacturer's protocol.

All assays were conducted in triplicate.

2.5. Confocal microscopy

Microscopic observation of the mature biofilms (37 days old) on membrane discs was performed in a laser scanning spectral confocal microscope (LEICA TSC SP5 X, Leica Microsystems Heidelberg GmbH, Germany) equipped with white laser, in the Research Infrastructures Area of University of Santiago de Compostela (Microscopy Unit). Samples were observed with an HCX PL APO CS 40.0 x1.25 OIL UV objective. Data were captured with Leica LAS AF software, in spatial scanning mode (XYZ) with a scan format resolution of 1024 x 1024 pixels. SABs were stained following the method described by Ref. [49] with concanavalin A, tetramethylrhodamine conjugate (lectin ConA-TMR) and fluorescein isothiocyanate isomer I (FITC) (Invitrogen). One image was captured on a random area around the centre of each biofilm. A hybrid detector (HyD) was used to obtain the emission signal from the biofilm sample: polysaccharides were recorded in the blue channel (ConA-TMR: excitation, 552 nm; emission, 578 nm), extracellular proteins were recorded in the red channel (FITC: excitation, 495 nm; emission, 525 nm) and chlorophyll autofluorescence was recorded in the green channel (excitation, 664 nm; emission, 725 nm). The signal of chlorophyll autofluorescence within the cells was used to obtain the cell count and average cell size. The images covered each an area of 30,303.84 μm^2 and were analysed using ImageJ 1.54 software.

2.6. PAM fluorometry

Chlorophyll *a* fluorescence images of the mature biofilms (37 days old) on membrane discs were captured using a Handy FluorCam FC 1000-H PAM (Pulse Amplitude Modulated) imaging fluorometer (Photon Systems Instruments, Czech Republic). The mean values of the whole biofilm surface were thus recorded for the parameters under study. The device uses a non-actinic light at 640 nm to record the minimum fluorescence (F_0), followed by a pulse of saturating actinic white light at 1046.00 μmol s^{-1} m^{-2} to record the maximum fluorescence (F_{max}). The samples were subjected to alternating pulses of actinic white light at 206.00 μmol s^{-1} and far-red light (740 nm) at 10.50 μmol s^{-1} to record other relevant parameters derived from the resulting Kautsky curve. The following parameters were determined, in addition to the F_0 and F_{max}: maximum quantum yield (QY_{max}) and light-adapted quantum yield (QY), non-photochemical quenching (NPQ), coefficient of photochemical quenching (qP) and fluorescence decline ratio (R_{df}). All fluorescence parameters were measured in relative units, with the exception of QY and QY_{max}, which ranged from 0 to 1.

2.7. Statistical analysis

The Kolmogorov-Smirnov test was used to test the normality of the data. As the wet biomass, the biochemical profile and the QY and qP parameters from the PAM fluorometry analysis were not normally distributed ($p \leq 0.05$), a non-parametric approach was adopted. Data regarding the daylight set-up (LDI and HDI) were compared using Wilcoxon test ($p \leq 0.05$). Data regarding the

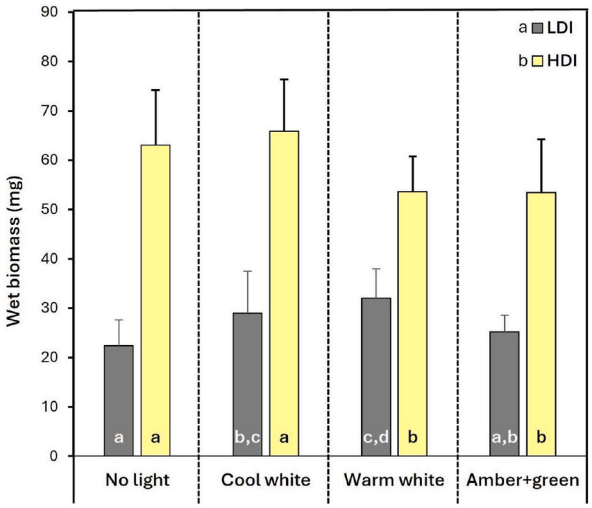

Fig. 2. Growth of subaerial biofilms (SABs) expressed as wet biomass (mg), under different ornamental lighting conditions. Bars indicate mean values and lines represent SDs. Different letters indicate significant differences in relation to ornamental illumination and the daylight scenario (LDI: low daylight illuminance; HDI: high daylight illuminance).

ornamental lighting conditions were compared using a Kruskal-Wallis test and a *post-hoc* Conover's test with Benjamini-Yekutieli adjustment ($p \leq 0.05$).

A Pearsons correlation matrix was constructed ($p \leq 0.05$) and principal Component Analysis (PCA) was performed to examine the relationship between wet biomass (WB) and the PAM fluorometry parameters.

All statistical analyses were conducted using R software (version 4.4.2) and R Studio (version 2024.12.1 + 563).

3. Results

3.1. Biofilm growth

Growth of the SABs under the ornamental light regimes in both daylight scenarios is summarised in Fig. 2. Regardless of the type of ornamental lighting, the wet biomass yield was significantly greater under HDI (58.96 ± 11.15 mg) than under LDI (27.18 ± 6.84 mg). In the LDI set-up, biomass production was significantly higher under both ornamental white lights (29.02 ± 8.48 mg under cool white and 32.01 ± 5.95 mg under warm white) than under no light at night (22.41 ± 5.18 mg). There was no difference in biomass production under the amber + green light (25.26 ± 3.30 mg) and the no light and the cool white light conditions. In the HDI set-up, no light and exposure to cool white light yielded significantly more wet biomass (63.09 ± 11.16 mg and 65,90 ± 10.46 mg, respectively) than exposure to warm white and amber + green lights (53.58 ± 7.18 mg and 53.42 ± 10.77 mg, respectively).

3.2. Species diversity

The taxonomic identification by examination of morphological characters of the inoculum of phototrophs mainly revealed the presence of green algae, such as *Chlorella vulgaris* Beijerinck (44.14 %), *Klebsormidium flaccidum* (Kützing) P.C. Silva, Mattox & W.H. Blackwell (19.99 %) and some *Chlamydomonas* spp. (2.63 %), *Coelastrella terrestris* (Reisigl) Hegewald & N. Hanagata (2.02 %), *Ettlia* sp. (2.71 %), *Monoraphidium obtusum* (Korshikov) Komárková-Legnerová (1.81 %), *Scenedesmus* sp. (4.56 %) and *Tetradesmus obliquus* (Turpin) M.J. Wynne (2.63 %). There was also a notable presence of cyanobacteria belonging to *Synechocystis* spp. 17.66 %) and some *Pseudoanabaena* spp. (1.84 %). Light-triggered changes in the relative abundance of the species in the SABs formed under the combination of daylight and artificial light at night are shown in Table 1. The three ornamental LED lighting conditions yielded minimal changes in the relative abundance of the species in the SABs relative to no light (control). Significant differences were only observed in the LDI set-up, with warm white and amber + green lights affecting green algae and by cool white light affecting cyanobacteria. *Chlorella vulgaris*, the most abundant species in the SABs comprising around 50 % of the specifical abundance, was not affected by the ornamental lights, but was two times more abundant in the HDI set-up (23.68 %) than in the LDI set-up (10.88 %). Under LDI and compared with no light, the proportion of *Klebsormidium flaccidum* significantly decreased from 14.61 % to 6.09 % under warm white light and to 8.82 % under amber + green light Moreover, generally decreased from LDI to HDI between 3.27 % and 13.58 % depending on the ornamental light applied. The relative abundance of *Ettlia* sp. also differed significantly, between the no light condition (1.31 %) and the (amber + green light condition (3.26 %). The relative abundance of *Monoraphidium obtusum* and of *Coelastrella terrestris* increased significantly from respectively 0.72 % and 0.51 % (no light) to 2.15 % and 2.34 % (warm white light). The relative

Table 1
Relative abundance (in %) of the different species detected in the subaerial biofilms (SABs) under combined low and high daylight illuminance (LDI and HDI) and ornamental LED lighting conditions (no light, cool white, warm white and amber + green lights). Statistically significant differences (at $p < 0.05$) relative to the control (no light) are indicated by (*).

Species	Daylight	No light		Cool white		Warm white		Amber + green	
		Mean	SD	Mean	SD	Mean	SD	Mean	SD
Chlorella vulgaris	LDI	**52.40**	12.33	**55.91**	7.47	**47.05**	8.11	**43.60**	5.40
	HDI	**63.80**	9.47	**66.78**	6.67	**63.53**	7.48	**67.28**	0.82
Klebsormidium flaccidum	LDI	**14.61**	1.58	**16.08**	0.17	**6.09***	1.54	**8.82***	5.69
	HDI	**2.60**	1.65	**2.50**	0.70	**3.49**	0.67	**5.55**	2.60
Scenedesmus spp.	LDI	**1.80**	0.75	**3.49**	1.91	**2.88**	1.24	**3.05**	1.00
	HDI	**1.95**	0.80	**2.00**	0.01	**1.82**	1.56	**2.22**	1.10
Ettlia spp.	LDI	**1.31**	2.27	**0.76**	0.39	**1.74**	0.42	**3.26***	0.29
	HDI	**1.54**	0.33	**0.69**	0.70	**1.23**	0.37	**1.39**	0.04
Tetradesmus obliquus	LDI	**0.79**	0.43	**2.82**	2.34	**2.36**	0.82	**2.63**	1.63
	HDI	**0.98**	0.92	**1.17**	0.21	**1.37**	0.87	**1.33**	0.63
Monoraphidium obtusum	LDI	**0.72**	0.06	**1.08**	0.70	**2.15***	0.70	**1.81**	0.58
	HDI	**1.07**	0.54	**1.03**	0.03	**1.94**	0.42	**1.05**	0.30
Coelastrella terrestris	LDI	**0.51**	0.88	**1.01**	0.66	**2.34***	1.22	**1.69**	0.66
	HDI	**1.46**	0.71	**0.66**	0.59	**1.87**	0.43	**1.65**	0.84
Chlamydomonas spp.	LDI	**0.49**	0.32	**0.79**	0.15	**0.71**	0.40	**0.77**	0.79
	HDI	**0.73**	0.37	**0.77**	0.52	**1.26**	0.71	**0.77**	0.18
Synechocystis spp.	LDI	**27.39**	6.74	**16.51***	2.41	**33.53**	5.91	**33.89**	1.51
	HDI	**25.77**	11.85	**24.37**	9.01	**23.43**	5.62	**18.69**	1.45
Pseudoanabaena sp.	LDI	**<0.01**	0.00	**1.56***	1.13	**1.16**	0.13	**0.47**	0.50
	HDI	**0.11**	0.11	**0.03**	0.05	**0.07**	0.07	**0.08**	0.04

abundance of *Synechocystis* spp. differed significantly between the no light (27.39 %) and cool white light (16.51 %) conditions. The presence of *Pseudoanabaena* sp. was almost negligible in the unlit control, but the relative abundance was significantly higher under cool white light (1.56 %).

3.3. Biochemical profile and confocal microscopy

Fig. 3 presents the effects of different night-time ornamental light regimes on the contents of chlorophyll *a* (Fig. 3a) and chlorophyll *b* (Fig. 3b), exopolysaccharides (Fig. 3c) and ATP (Fig. 3d).

LDI favoured an increase in chlorophyll *a* (1.51 ± 0.38 mg g^{-1} SAB) while HDI favoured an increase in chlorophyll *b* (1.03 ± 0.27 mg g^{-1} SAB). In the LDI set-up, the warm white light caused a significant reduction in chlorophyll *a* (1.12 ± 0.11 mg g^{-1} SAB) relative to the no light control (1.84 ± 0.50 mg g^{-1} SAB). There were no significant differences in chlorophyll *a* concentration in the HDI scenario, despite the increase observed under the warm white and amber + green lights. Similarly, there were no significant differences in chlorophyll *b* concentrations between the ornamental lights in either of the two daylight conditions.

The protein content in the EPS was below 5 μg mL^{-1} in all of the samples analysed. Thus, reliable quantification was not possible with the technique used due to the low protein content of the matrix. Thus, the analysis focused exclusively on the exopolysaccharide fraction of the EPS.

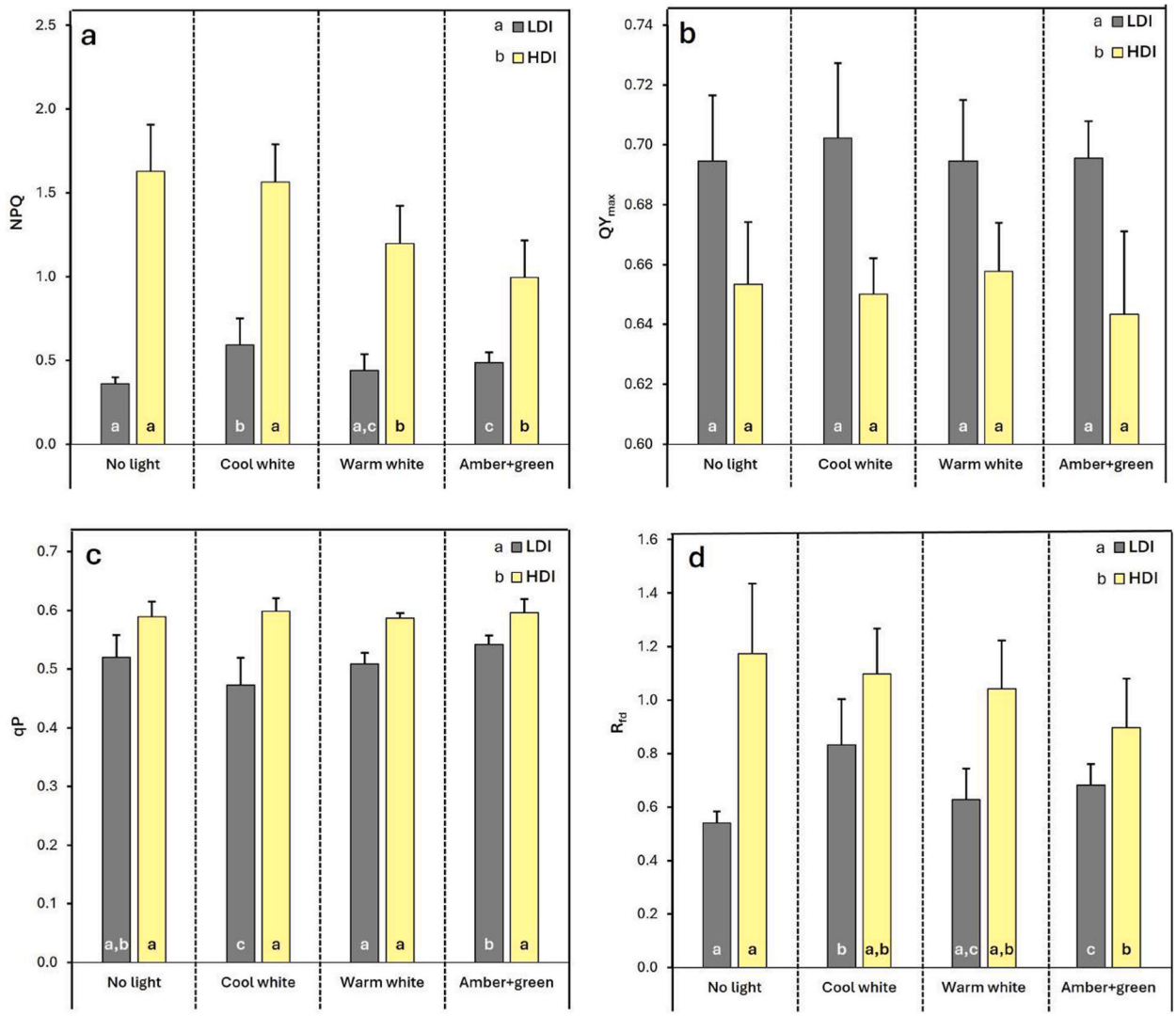

Fig. 3. Biochemical profile of subaerial biofilms (SABs) under the different ornamental lighting conditions: a) Chlorophyll *a* content (mg g^{-1} SAB), b) Chlorophyll *b* content (mg g^{-1} SAB), c) exopolysaccharide content (mg g^{-1} SAB) and d) ATP content (pmol μg^{-1} SAB). Bars indicate mean values and lines represent SD. Different letters indicate significant differences in relation to ornamental illumination and the daylight scenario (LDI: Low Daylight Illuminance; HDI: High Daylight Illuminance).

The exopolysaccharide content was significantly lower in the HDI set-up (18.35 ± 5.52 mg mg^{-1} SAB) than in the LDI set-up (101.89 ± 59.73 mg mg^{-1} SAB). In LDI a reduction in exopolysaccharides was detected under warm white (85.71 ± 24.08 mg EPS mg^{-1} SAB) and amber + green (31.34 ± 3.17 mg mg^{-1} SAB) lights, with the latter being significantly lower than in the no light control (154.46 ± 70.83 mg mg^{-1} SAB). In the HDI set-up, there were no significant differences between the light conditions tested.

Finally, the ATP content was significantly higher under HDI (467.24 ± 216.56 pmol ATP mg^{-1} SAB) than under LDI (270.90 ± 155.25 pmol ATP mg^{-1} SAB), in which no significant differences were detected. Under HDI, the amber + green light (569.23 ± 161.53 pmol ATP mg^{-1} SAB) increased the ATP concentration significantly, relative to the no light control (307.45 ± 122.77 pmol ATP mg^{-1} SAB).

The average contents of polysaccharides, extracellular proteins and chlorophyll in the confocal microscopy images, as well as the cell count per μm^2 and the average cell size, are shown in Fig. 4. Ornamental lighting conditions caused significant differences in all parameters examined by confocal microscopy in the LDI scenario but not in the HDI scenario.

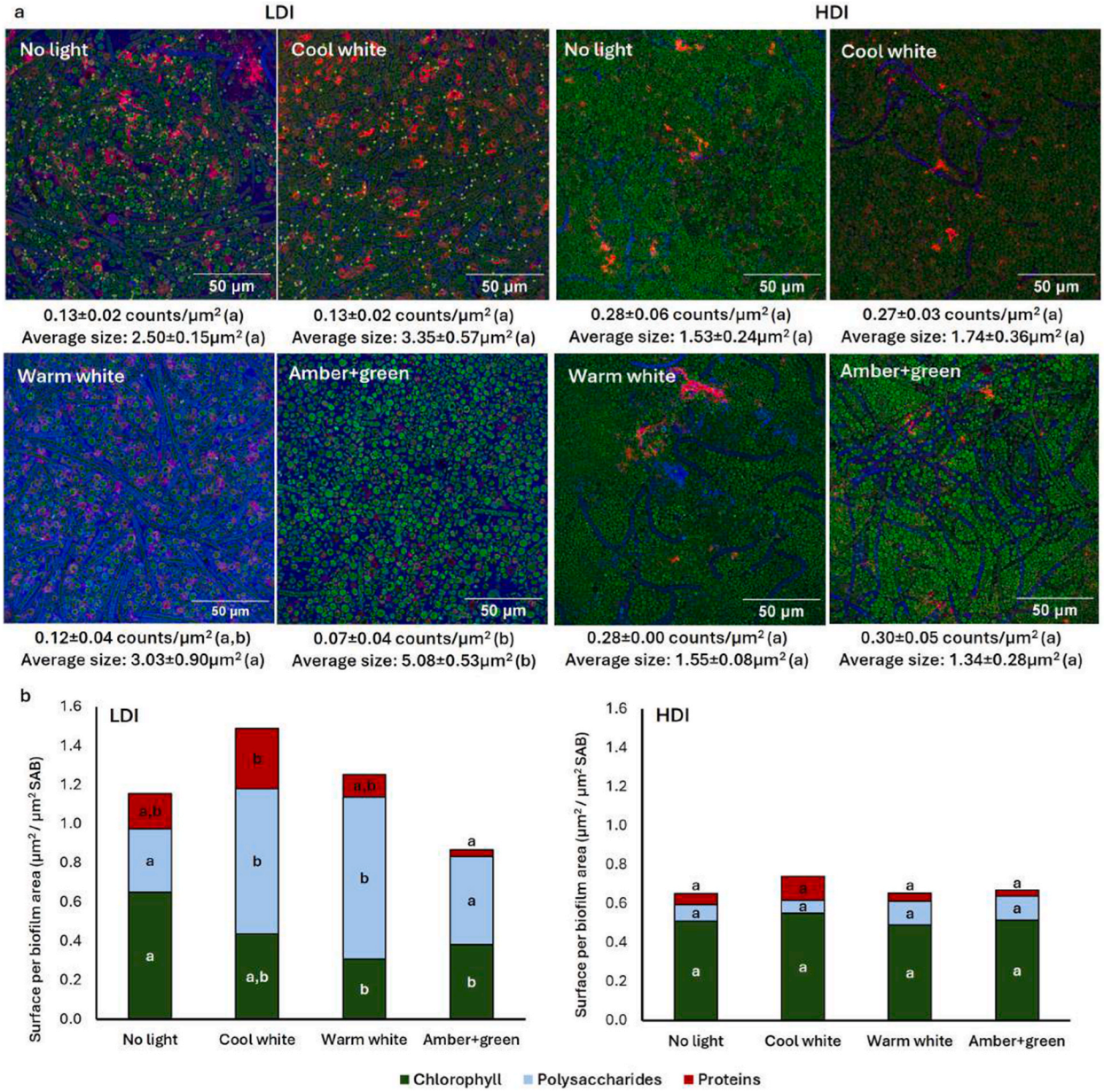

Fig. 4. a) Confocal microscope images of subaerial biofilms (SABs) under the different ornamental lighting conditions (green indicates chlorophylls; blue indicates polysaccharides; and red. indicates proteins). b) Surface area occupied by each component in the images of the SAB captured by confocal microscopy. Different letters indicate significant differences relative to ornamental illumination for the same daylight illuminance (LDI: low daylight illuminance; HDI: high daylight illuminance).

In the LDI set-up, the algal cells were more separated, with a lower cell density per μm^2 (0.07–0.13 counts μm^{-2}) than in the HDI set-up (0.27–0.30 counts μm^{-2}). Considering the differences between the ornamental lighting conditions in LDI, there was a significant reduction in cell counts per surface area under the amber + green light (0.07 ± 0.04 counts μm^{-2}) than in the no light control (0.13 ± 0.02 counts μm^{-2}). In terms of mean average cell size in the LDI scenario, amber + green light produced a significantly greater increase in average cell size (5.08 ± 0.53 μm^2) than both white lights (3.35 ± 0.57 μm^2, cool white and 3.03 ± 0.90 μm^2, warm white) and the no light control (2.50 ± 0.15 μm^2). The relative abundance of filamentous algal cells was higher in the LDI set-up than in the HDI set-up (Fig. 4a). According to the taxonomic data, *Klebsormidium flaccidum* was the only filamentous alga present in the SABs. Remains of membranes and walls (indicating polysaccharides) without chlorophyll were observed in the HDI set-up, following the reduction in the relative abundance of this species in the SAB observed in the taxonomic analysis (Table 1).

The polysaccharide content was lower in the HDI set-up (0.10 ± 0.02 μm^2 μm^{-2} SAB) than in the LDI scenario (0.59 ± 0.24 μm^2 μm^{-2} SAB). In the LDI set-up, the surface area occupied by polysaccharides was higher in the cool white light (0.74 ± 0.30 μm^2 μm^{-2} SAB) and the warm white light (0.83 ± 0.10 μm^2 μm^{-2} SAB) conditions than in the amber + green (0.45 ± 0.25 μm^2 μm^{-2} SAB) light and the no light control (0.32 ± 0.30 μm^2 μm^{-2} SAB) conditions. The ornamental lighting conditions yielded a significant reduction in the quantity of chlorophyll per biofilm surface area in the LDI set-up, relative to the no light control (0.65 ± 0.33 μm^2 μm^{-2} SAB) under the warm white light (0.31 ± 0.14 μm^2 μm^{-2} SAB) and the amber + green light (0.38 ± 0.15 μm^2 μm^{-2} SAB) conditions. Proteins were

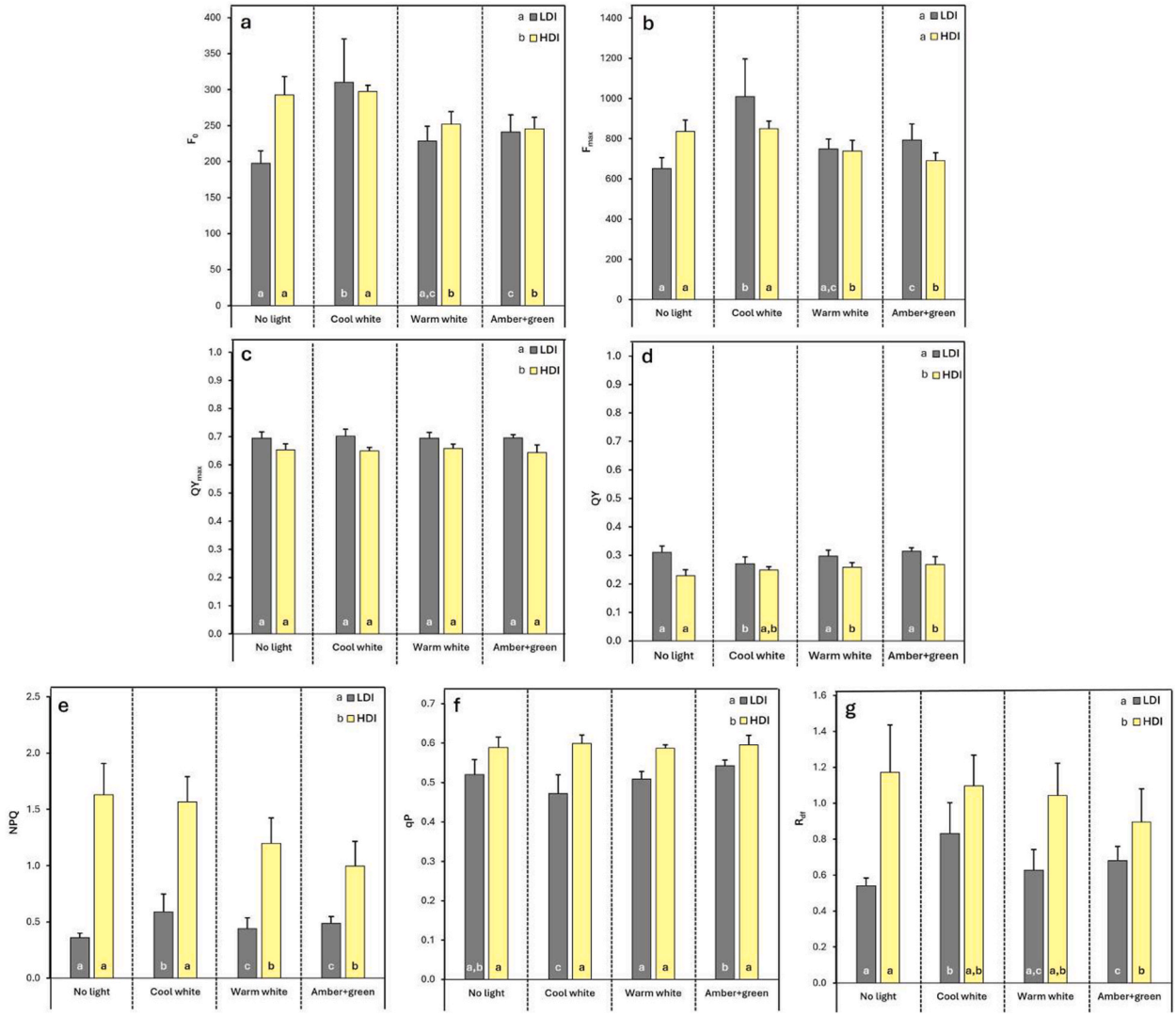

Fig. 5. PAM fluorometry results for analysis of subaerial biofilms (SABs) under the different ornamental lighting conditions: a) minimum fluorescence (F_0), b) maximum fluorescence (F_{max}), c) maximum quantum yield (QY_{max}), d) light-adapted quantum yield (QY), e) non-photochemical quenching (NPQ), f) photochemical quenching (qP), and g) fluorescence decline ratio (R_{df}). Bars indicate mean values and lines represent SD. Different letters indicate significant differences in relation to ornamental illumination and the daylight scenario (LDI: low daylight illuminance; HDI: high daylight illuminance).

significantly more affected by cool white light (0.31 ± 0.26 $\mu m^2\ \mu m^{-2}$ SAB) than by the no light condition (0.18 ± 0.06 $\mu m^2\ \mu m^{-2}$ SAB) in the LDI set-up (Fig. 4b).

3.4. PAM fluometry

The minimum and maximum fluorescence (F_0 and F_{max}) values exhibited a similar pattern to that observed for biomass in both the LDI and HDI conditions (Fig. 5a and b).

In the LDI set-up, all ornamental LED light conditions caused an increase in F_0 and F_{max}, but only the cool white light (310.25 ± 60.40 for F_0 and 1010.44 ± 186.58 for F_m) and the amber + green light (241.25 ± 23.89 for F_0 and 792.93 ± 81.37 for F_m) yielded significant differences relative to the no light control (197.70 ± 17.14 for F_0 and 651.70 ± 53.91 for F_m). No significant differences in QY_{max} were observed for the illumination conditions in either the LDI or HDI set-up (Fig. 5c). However, the average QY_{max} values were significantly higher in the LDI set-up (0.70 ± 0.02) than in the HDI set-up (0.65 ± 0.01). The light-adapted quantum yield (QY) was significantly lower under the cool white light (0.27 ± 0.03) than in the no light control (0.31 ± 0.02) in the LDI set-up. In the HDI set-up, the QY was higher in both the warm white (0.26 ± 0.02) and the amber + green light (0.27 ± 0.03) conditions than under the no light condition (0.23 ± 0.02).

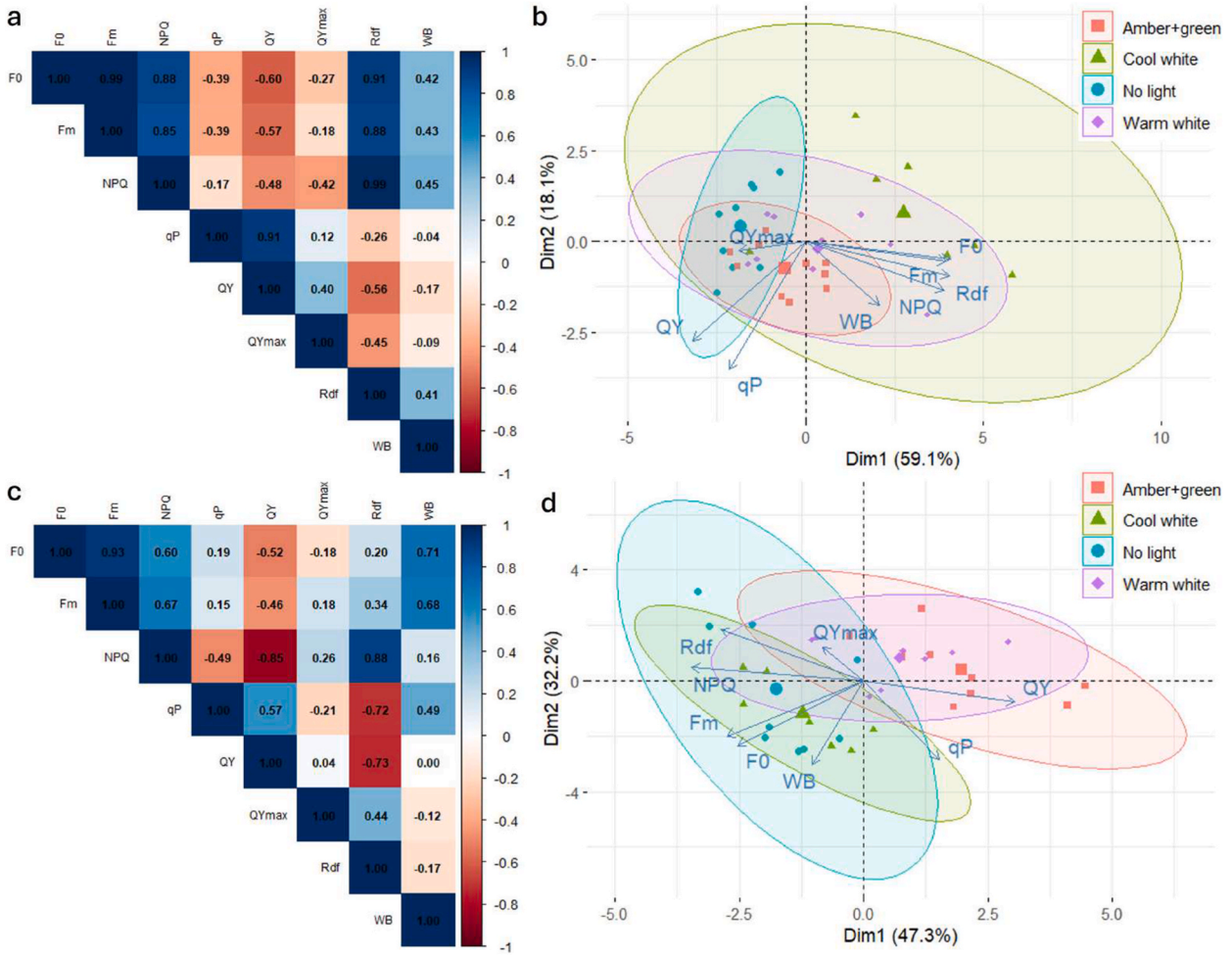

Fig. 6. a) Correlation matrix according to Pearson's test for the PAM fluorometry variables and the wet biomass (WB) of subaerial biofilms (SABs) under the different ornamental lighting conditions in the low daylight illuminance (LDI) set-up, b) Principal Component Analysis (PCA) plot for the PAM fluorometry variables and the wet biomass (WB) of subaerial biofilms (SABs) under the different ornamental lighting conditions in the low daylight illuminance (LDI) set-up, c) Correlation matrix according to Pearson's test for the PAM fluorometry variables and the wet biomass (WB) of subaerial biofilms (SABs) under the different ornamental lighting conditions in the high daylight illuminance (HDI) set-up and d) Principal Component Analysis (PCA) plot for the PAM fluorometry variables and the wet biomass (WB) of subaerial biofilms (SABs) under the different ornamental lighting conditions in the high daylight illuminance (HDI) set-up. The symbols indicate the position of each sample within the plot (large symbols indicate each centroids). Coloured ellipses are based on the centroids for each ornamental lighting condition. The arrows indicate the variables used for the PCA.

The non-photochemical quenching (NPQ) (Fig. 5d) was significantly higher in the LDI set-up with the cool white light (0.59 ± 0.16) and the amber + green light (0.49 ± 0.06) than in the no light control condition (0.36 ± 0.04). In the HDI set-up, the NPQ was significantly lower in the warm white light condition (1.20 ± 0.23) and the amber + green light (1.00 ± 0.22) condition than in the control condition. NQP was significantly higher in the HDI set-up (1.33 ± 0.35) than in the LDI set-up (0.47 ± 0.13).

The photochemical quenching coefficient (qP) was also higher in the HDI set-up (0.59 ± 0.02), in which no differences were found between conditions, than in the LDI set-up (0.51 ± 0.04) in which only the cool white light (0.47 ± 0.05) caused a significant reduction (Fig. 5e). Finally, the fluorescence decline ratio (R_{df}) (Fig. 5f) was significantly higher in the HDI set-up (1.05 ± 0.22) than in the LDI set-up (0.67 ± 0.15). In the LDI set-up, the R_{df} was higher in the cool white light (0.83 ± 0.04) and the amber + green light (0.68 ± 0.12) conditions than in the control condition. In the HDI set-up, only the amber + green light (0.90 ± 0.18) reduced the R_{df} relative to the no light control (1.17 ± 0.26).

A Pearson correlation matrix was constructed (Fig. 6a and c) and principal Component Analysis (PCA) (Fig. 6b and d) was conducted to examine the relationships between the wet biomass (WB) and the PAM fluorometry parameters.

The correlation matrix shows that wet biomass was positively correlated with F_0 ($r = 0.42$ in LDI and $r = 0.71$ in HDI) and F_m ($r = 0.43$ in LDI and $r = 0.68$ in HDI) in both daylight set-ups, although that correlation was stronger for HDI than for LDI. There was also a positive correlation between wet biomass and NPQ ($r = 0.45$) and R_{df} ($r = 0.41$) in the LDI set-up, but the correlation was weaker in the HDI set-up for NPQ ($r = 0.16$) and was negative for R_{df} ($r = -0.17$). qP and QY were negatively correlated with NPQ and R_{df} in both the LDI and HDI set-ups. qP was also negatively correlated with F_0 and F_m in LDI ($r = -0.39$), but the correlation was positive in HDI ($r = 0.19$ for F_0 and $r = 0.15$ for F_m). This was also observed with the correlation between QY_{max} and NPQ and R_{df}, which was negative in LDI ($r = -0.42$ for NPQ and $r = -0.45$ for R_{df}) and changed to positive in the HDI set-up ($r = 0.26$ for NPQ and $r = 0.44$ for R_{df}). Finally, Rfd was strongly and positively correlated with NPQ in both LDI ($r = 0.99$) and HDI ($r = 0.88$), and the relationship with WB was positive in LDI ($r = 0.41$) but negative in HDI ($r = -0.17$).

The first two dimensions of the PCA (Dim1 and Dim2) explained 77.2 % of the variance in the data in the LDI set-up (Dim1 = 59.1 % and Dim2 = 18.1 %) (Figs. 6b) and 79.5 % of the variance in the HDI set-up (Dim1 = 47.3 % and Dim2 = 32.2 %) (Fig. 6d). In the LDI set-up, the Dim2 mainly explained the no light control, whereas the Dim1 displacing the SABs subjected to ornamental lightning away from the control SABs, with F_0, F_m, NPQ, R_{fd} and WB being the main parameters causing the displacement. The PCA shows that in the LDI set-up the SABs subjected to amber + green ornamental lighting were more similar to the no light control, followed by the warm white light and the cool white light. However, in the HDI set-up, the PCA showed that the SABs under amber + green light were the most displaced from the no light control and the SABs under cool white light the most similar. For both warm white and amber + green lights, the Dim1 mainly explained the variance, with the QY parameter being the most important causing the displacement from the control. The SABs under amber + green light appear on opposing axes in the PCAs to the F_0, F_m, NPQ, R_{fd} and WB parameters in both the LDI and HDI conditions.

4. Discussion

4.1. Biofilm growth

Ornamental illumination of architectural heritage artificially increases the time that phototrophic colonisers are exposed to light and carry out photosynthesis. However, most of the literature regarding changes derived from different lighting regimes has focused on algal bioreactors.

In the present study, the use of both cool and warm white lights increased the wet biomass in the LDI set-up (Fig. 2a). A study by Ref. [50] investigating the effects of photoperiod duration under low light conditions (50 μmol s^{-1} m^{-2}, comparable to the LDI condition), revealed a gradual increase in the density of *Nannochloropsis* spp. cells as the photoperiod was increased from a 12:12 h light-dark cycle to an 18:6 h cycle, with a maximum observed under continuous illumination (24:0 h cycle). However, under higher light intensity (200 μmol s^{-1} m^{-2}, similar to the HDI condition), although the cell density was generally higher than at low light intensity (below 50 μmol s^{-1} m^{-2}), there were no significant differences between the 12:12 h and 18:6 h cycles, and continuous illumination caused a reduction in cell density. Similar findings to those observed in planktonic cultures (in bioreactors) have also been reported for biofilms [51]. found that the biomass of algal biofilms of *Chlorella vulgaris* was slightly but significantly higher under continuous illumination than under a 12:12 h cycle.

Nevertheless, it is not known whether variations in daylight illuminance interfere with the capacity of night-time lighting systems to generate the light-related stress that affects the growth and development of organisms. The use of amber + green light did not enhance wet biomass production of the SABs in the LDI, unlike the cool and warm white lights tested. Moreover, in the HDI set-up the amber + green light resulted in a reduction in both wet biomass of the SABs (Fig. 2), suggesting a potential biostatic effect at both levels of sunlight intensity. Light in the 500–600 nm range (green to yellow/amber) is conventionally regarded as less efficient for photosynthesis, as it results in lower CO_2 assimilation per mole of photons than wavelengths in the 450–500 nm (blue) and 600–750 nm (orange to red) ranges. This is consistent with the peak absorption spectra of chlorophyll, in which blue and red light are most effectively used for photosynthetic activity (see e.g.[52]). Cultures of *Chlorella vulgaris* grown in a column bioreactor under continuous monochromatic illumination (500–2000 lx) exhibited lower specific growth rates and cell concentrations when exposed to green light (510–540 nm) than when exposed to red (650–680 nm) or blue (440–470 nm) light [53] Similar findings were reported by [54], in a study in which the dry mass density of *Chlorella vulgaris* cultures subjected to continuous monochromatic light (150 μmol s^{-1} m^{-2}) was lower after exposure to yellow (590 nm) and green (525 nm) light than after exposure to blue (467 nm), red (625 nm) and white light.

Although warm light produced similar positive results to amber + green light in the HDI in terms of biomass, warm white light

yielded the greatest amount of wet biomass in the LDI (Fig. 2a). These inconsistencies between the two types of daylight illuminance may hinder the potential use of warm white light to reduce the development of SABs [55] demonstrated that higher cell density was reached in *Chlorella vulgaris* cultures grown under warm white light with an 18:8 h photoperiod than in those exposed to cooler white light, regardless of the light intensity (50, 80, or 110 μmol s^{-1} m^{-2}). However [56], reported no significant difference in dry density of *Chlorella vulgaris* cultures grown under cool white (6500K) and warm white (3200K) light at an intensity of 50 μmol s^{-1} m^{-2}. The findings suggest that the effects of white light spectra on microalgal growth are influenced by other culture conditions beyond light quality alone.

The phototrophic community within the SABs underwent changes in response to both sunlight intensity and the spectral characteristics of the ornamental lighting applied in the experiment. Biofouling tends to be more prevalent on north- and west-facing facades, which in the Atlantic region are typically more shaded and humid [57] Additionally, the diversity of colonising species is generally higher on surfaces that receive less direct sunlight, whether due to orientation or external shading [58]. In the present study, humidity was not a limiting factor, as culture on the agar plates ensured continuous water availability. Consequently, higher solar irradiation resulted in increased biomass production (Fig. 2a), contrary to expectations for facades exposed to strong insolation. This also applies to species diversity, given that the system is closed, and the species composition remained unchanged, with only the relative abundance varying under different light regimes.

4.2. Species diversity

The most abundant species in the SABs generated were *Chlorella vulgaris* (Chlorophyta)*, Klebsormidium flaccidum* (Charophyta) and *Synechocystis* sp. (Cyanobacteriota) (Table 1). *Chlorella vulgaris,* a coccoid unicellular green alga, is one of the most important initial pioneering species [60] and it is found in Galicia (NW Spain) in heritage constructions built in granite ([61,62]), in limestone buildings in France [63], in marble fountains in Bratislava [64] and even on architectural concrete ([65,66]). The filamentous green alga *Klebsormidium flaccidum* is commonly associated with mineral substrates on building facades [59]. This cosmopolitan species is found across various lithotypes [67] and it has specifically been reported on granite buildings in Galicia (NW Spain) [68] and as endolithic growth in the granite masonry of the Ordem de São Francisco Church in Porto (Portugal) ([69,70]. In Europe, members of the phylum Cyanobacteriota are generally less abundant than green algae in phototrophic biofilms [71]. However, the genus *Synechocystis* has been detected on various lithic substrates, including travertine in Italy [72], calcareous substrates such as mortar or limestone [73] and in granite in Portugal [69].

Chlorella vulgaris was much less abundant in the LDI set-up (50.07 μmol s^{-1} m^{-2}) than in the HDI set-up (252.59 μmol s^{-1} m^{-2}), with the biomass increasing by between 10.88 % and 23.68 % depending on the ornamental lighting condition (Table 1). In a closed bioreactor, *Chlorella vulgaris* increased its growth rate consistently between 130 and 520 μmol s^{-1} m^{-2} [74], revealing the capacity of this species to thrive under higher insolation. By contrast, the presence of *Klebsormidium flaccidum* was found to be lower in the HDI than in the LDI set-up [75]. showed that the growth rate of the related species *Klebsormidium dissectum* was maximum at 30 μmol s^{-1} m^{-2} and then declined when the light intensity was increased to 120 μmol s^{-1} m^{-2}. Although *K. flaccidum* seems to prefer lower light intensity similar to that in shaded areas of facades, the presence of ornamental warm white and amber + green ornamental lighting caused a decrease in abundance of the species in the LDI set-up (Table 1). As a member of the streptophyte clade (a monophyletic group encompassing terrestrial plants and charophyte algae) the response of *Klebsormidium* spp. to variations in light spectra is expected to differ from that of the other microalgae and may exhibit similarities to higher plants. Members of the *Klebsormidium* genus possess blue-sensitive phototropins (photoreceptor proteins involved in phototropic responses) that are more closely related to those found in higher plants than to those found in other green algae [76]. Algal phototropins appear to regulate fewer key physiological functions than their plant counterparts [77]. This distinction may be particularly important when considering the different contribution of blue wavelengths under the various ornamental lighting conditions tested.

The reduction in *Klebsormidium flaccidum* by warm white and amber + green light in the LDI scenario is particularly interesting from a conservation standpoint, considering the capacity of the filaments for endolithic growth ([69,78]) filling cracks in the substrate which could become source mechanical stress resulting in the loss of cohesion, rupture or disintegration by mechanical pressure ([50, 79]).

Nonetheless, some green algal species can utilize the amber + green light more effectively than others for growth. Although not one of the predominant species in the SABs, the relative abundance of *Ettlia* sp. increased by 1.96 % under amber + green light conditions, relative the no light control in the LDI scenario [80]. showed that members of the genus *Ettlia* can grow effectively under continuous monochromatic green LED light, yielding the same biomass as when grown under monochromatic blue or red lights and outcompeting *Chlorella vulgaris* when present in mixed cultures. While species of the genus *Ettlia* are primarily associated with soil environments, they have also been detected on monuments and stone walls, albeit in low abundance (see e.g. Refs. [34,62,81]).

The abundance of cyanobacteria in the SABs was not affected by exposure to the amber + green light, although previous studies showed higher DNA counts [47] and peptides of cyanobacterial origin in phototrophic biofilms exposed to amber + green light than in films exposure to other white lights [34]. [82] suggested that nocturnal green lighting used to illuminate the stone walls of a millennial mausoleum in Shaanxi (China) affected the biodeterioration caused by metabolic activity of cyanobacteria, by reducing the production of lactic and citric acids. Cyanobacteriota have accessory pigments such as phycocyanins and phycoerythrins that absorb light at 610–625 nm and 490–570 nm [27]. Cyanobacteria possessing these pigments are more likely to be found on the surfaces of caves illuminated by warm light (which usually peaks around 600 nm due to the low blue component) [83]. However, in the present study no significant changes in cyanobacterial abundance were observed in areas exposed to warm light. Instead, a reduction in the abundance of *Synechocystis* sp. was noted under cool white light. This finding is consistent with previous research demonstrating that blue light

can have an inhibitory effect on *Synechocystis* sp. PCC 6803 [84], which is particularly relevant given that the cool white light used in this study peaked at 457 nm.

4.3. Biochemical profile and confocal microscopy

The biochemical profile of the SABs was influenced by ornamental lighting in the LDI set-up. However, no significant alterations were observed in the HDI set-up (Fig. 3), suggesting that the increased solar intensity during the day had a greater effect than any biochemical changes induced by nocturnal ornamental lighting. The chlorophyll *a* content of the SABs was reduced by ornamental lighting in the LDI set-up, whereas chlorophyll *b* remained unchanged. However, the reduction in chlorophyll *a* in the LDI set-up was only statistically significant for the warm white light condition. In a study involving *Nannochloropsis* sp. cultures, the chlorophyll *a* content decreased when the proportion of red wavelengths to blue wavelengths was increased [85]. The increase in the proportion of red light would cause a decrease in the CCT, thus resulting in a warmer white light.

In the previously mentioned study [56] cultures of *Chlorella vulgaris* produced more chlorophyll *a* than chlorophyll *b*, regardless of light quality or light intensity. The present findings show that under higher solar irradiance (HDI set-up), the concentration of chlorophyll *a* is reduced (Fig. 3a) but the concentration of chlorophyll *b* increases (Fig. 3b), regardless of the impact of ornamental lighting.

EPS production tends to be higher on sunny surfaces that on shaded surfaces, to protect cells from adverse conditions (see e.g. Refs. [24,86]) [87]. reported that the cyanobacteria *Microcoleus vaginatus* produced more EPS (in the form of polysaccharides) in a culture when the light intensity was increased from 4 to 80 μmol s^{-1} m-2. However, in a culture of the green alga *Dictyosphaerium chlorelloides* EPS production increased with light intensity at between 11.9 and 50.3 μmol s^{-1} m^{-2} (at the same light intensity as the LDI set-up) and then decreased at 68.6 μmol s^{-1} m^{-2} [88]. In the present study, the SABs produced a lower amount of exopolysaccharides (both in the direct determination and the confocal images, Figs. 3c and 5b) in the HDI set-up than in the LDI set-up. These findings suggest that higher light intensity may impede exopolysaccharide production, at least under laboratory conditions. The methods used to quantify exopolysaccharides yielded different results in response to ornamental lighting in the LDI scenario. Direct quantification indicated that the highest concentration of polysaccharide occurred in the control group without night-time lighting, with values undistinguishable from those observed under cool and warm white lights (Fig. 3c). Conversely, confocal microscopy analysis revealed that the exopolysaccharide concentration was higher under these two lighting conditions, than in the control, in which exopolysaccharide levels were lowest (Fig. 5b). This discrepancy may be attributed to variations in the spatial distribution of exopolysaccharides within the biofilm matrix, which exhibits some heterogeneity across three dimensions [89], as confocal microscopy measures polysaccharides in a specific area and depth whereas the direct determination quantifies the total amount in the SAB. The amber + green ornamental lighting condition produced a consistent response across both quantification methods, with exopolysaccharide production remaining low, both in direct determination (compared to the no-light control and the two white light conditions, Fig. 3c) and in confocal microscopy (relative to the two white lights and similar to the no-light control, Fig. 4b).

Confocal imaging analysis also revealed that extracellular protein levels were lowest under amber + green lighting. Light wavelength is known to modulate extracellular protein production, as demonstrated in previous studies in which exposure to red (630–675 nm) and in particular to blue (460–475 nm) light led to greater accumulation of both intracellular and extracellular proteins than exposure to white light in multi-species algal-bacterial consortia [90]. Similarly, in the present study, the higher proportion of blue wavelengths in the ornamental cool white light was associated with an increased proportion of extracellular proteins under the test conditions. The low levels of extracellular protein produced under the amber + green ornamental lights may be an important factor in controlling the colonization of the architectural heritage. Indeed [91], reported that the protein secreted by the green alga *Botryococcus braunii* accounted for strong adhesion of the cells to glass fibre, and the same protein has been reported to increase hydrophobicity in algal biofilms by cation bonding ([92,93]).

Although the biochemical profile was not affected by the ornamental lights tested in the HDI set-up, the amber + green light increased the ATP content of the SABs relative to the other ornamental lighting conditions (Fig. 3d). This can be tentatively attributed to the fact that light-induced stress at amber + green wavelengths is unable to efficiently drive photosynthesis at night-time. ATP is necessary to maintain proteostasis, fuelling protein synthesis and repair [94], and the increase in ATP content could therefore indicate an increase in protein metabolism. Indeed, previous studies investigated the effect of ornamental lighting in the proteome of SABs and found that exposure to amber + green light increased protein metabolism and even increased heat shock proteins HSP70 and HSP90, which is a sign of oxidative stress [34].

4.4. PAM fluorometry

PAM fluorometry was conducted in this study to examine changes in light use by SABs under nocturnal lighting. The correlation matrix (Fig. 6a and c) revealed a positive correlation between the wet biomass (Fig. 2) of SABs and both minimum (F_0) (Fig. 5a) and maximum (F_m) (Fig. 5b) fluorescence, with the relationship becoming strengthened in the HDI relative to the LDI condition. This suggests that under LDI, ornamental lighting exerts a greater influence on the direct correlation between biomass and fluorescence. This may have a stronger impact on biofilm physiology, consistent with the observed biochemical profile changes (Figs. 3 and 4). Measuring F_0 (as well as F_m) is sometimes considered a suitable in situ proxy method of estimating algal biomass (see e.g Ref. [95]., although the reliability of the method can be affected by external factors [96] such as, in this case, ornamental lighting.

The PCA plots (Fig. 6b and) revealed that the use amber + green light for ornamental illumination shifted the SABs in LDI opposing the F_0, F_m, NPQ and R_{df} parameters, driving the SABs under cool and warm white light to deviate from the control SABs. In the LDI set-

up, the F_0 was higher under amber + green than under warm white light, despite the lower amount of biomass produced (Fig. 2). It has been shown that F_0 increases at sub-optimal conditions [97], which supports the potential of amber + green as a biostatic light. In the PCA of the HDI set-up, the F_0, F_m, NPQ and R_{df} parameters were on opposing axes to the SABs under amber + green light but were more scattered along the y-axis (Dim2). Thus, the effect of the ornamental lighting at night loses strength against the higher solar irradiance during the day.

The quantum yield of the SABs was lower in the HDI set-up than in the LDI set-up, indicating the efficiency with which absorbed light is capable of driving photochemistry in both the maximum and light adapted photosystem II (PSII). Similarly [95], reported that maximum quantum yield in microphytobenthos was negatively correlated with ambient irradiance ranging from 200 to 1000 μmol s^{-1} m^{-2}. However, the ornamental lighting conditions did not modify the QY_{max} (Fig. 5c) following the conclusions of [98] who deemed that QY_{max} was not a wavelength-dependent parameter (between 440 and 625 nm) in a natural phytoplankton community. However, under the amber + green light, the light adapted quantum yield (QY) was higher in both daylight scenarios than in the no light control. Cultivation of *Dunaliella bardawil* under monochromatic red and blue light affected the QY_{max} and QY of cultures relative to cultivation under white light, indicating that changes in from a white light spectra can cause an increase in quantum yield. Moreover [99], found that green light can penetrate deeper into higher plant leaves that blue or red light in strong white light, thus increasing leaf photosynthesis to a greater extent. SABs consist of a structured community of cells that can reach a considerable thickness, particularly when grown in the laboratory. For example [100], produced biofilms of *Chlorella sorokiniana* of thickness up to 847 μm. Thus, mechanisms such as that occurring in leaves (see Ref. [101]) may explain the higher QY after exposure to daylight observed under amber + green light (Fig. 5d) despite the lower biomass yield.

In the non-photochemical quenching (NPQ) mechanism, the excessive excitation energy that cannot be used for photosynthesis is dissipated as heat [102]. The NPQ was higher in the HDI set-up than in the LDI set-up for all the ornamental light conditions tested (Fig. 5e). Indeed, increases in non-photochemical quenching has been observed on increasing the irradiance from 0 to 400 μmol s^{-1} m^{-2} [103] and from 50 to 2000 μmol s^{-1} m^{-2} [104] in several green macroalga species. Contrary to NPQ, photochemical quenching (qP) is proportional to the photon energy captured by open PSII reaction centres and dissipated via photosynthetic electron transport [105]. The qP tends to decrease when photosynthesis is saturated, as shown by Ref. [106] in cultures of the microalga *Koliella antarctica* from 0 to 1000 μmol s^{-1} m^{-2}. However, in the present study, the qP was higher in the SABs formed in the HDI set-up than in the LDI set-up (Fig. 5f), possibly indicating that the photosynthetic machinery of the SABs was not saturated at the levels of daylight irradiance tested.

Finally, parameter R_{df}, also termed the "vitality index", is considered a good measure of stress effects on the PSII [107]. The R_{df} was higher in the SABs formed in the HDI scenario than in those formed in the LDI set-up, further indicating that the HDI irradiance did not lead to saturation or photoinhibition. In the LDI set-up, the use of ornamental lighting increased the R_{df}, particularly under cool white light. However, the use of amber + green light caused a significant reduction in R_{df} relative to the no light control and the other ornamental lighting conditions tested (Fig. 5g). To the best of our knowledge, light intensity and light quality have not been shown to affect the vitality of green algae. [108] showed that the cyanobacteria *Anabaena* CPB4337 and the green alga *P. subcapitata* (grown at an irradiance of 65 μmol s^{-1} m^{-2}) suffered a decrease in R_{df}, indicating signs of stress, when subjected to high concentrations of CeO_2 nanoparticles. Similarly to the present study, the decrease in R_{df} was followed by a decrease in NPQ, and both parameters were positively correlated.

5. Conclusions

The use of nocturnal ornamental illumination has been proposed as a potential biostatic strategy to manage phototrophic colonization on architectural heritage. However, the extent to which variations in daylight illuminance modulate the efficacy of nocturnal lighting in inducing light-related stress responses that influence the growth and development of phototrophic organisms remains unknown.

In the LDI set-up, exposure to both types of white light increased biomass production in the SABs, whereas exposure to amber + green light did not cause any difference in biomass production relative to the no light control. In the HDI set-up, the biomass of the SABs was lower in both the warm white light and the amber + green light conditions than in the cool white light and the no light conditions. The distribution of the species within the SAB were different in the LDI and HDI conditions, but the ornamental lighting barely altered the species composition. The relative abundance of *Chlorella vulgaris* increased under all ornamental lighting conditions in the HDI set-up. The relative abundance of *K. flaccidum* was lower in the HDI than in the LDI set-up; in the LDI set-up, the relative abundance was lower after exposure to warm white and the amber + green lights than after exposure to the other ornamental lighting conditions.

Nocturnal ornamental illumination did not alter the biochemical profile (in terms of contents of chlorophyll, exopolysaccharides and extracellular proteins) in the HDI set-up. However, in the LDI set-up, exposure to amber + green light reduced the exopolysaccharide content in the extracellular matrix, detected by both direct quantification and confocal microscopy. Confocal microscopy analysis also revealed that exposure to the amber + green ornamental light reduced the extracellular proteins compared to the white lights tested.

Analysis of the samples by PAM fluorometry showed that the effect of the ornamental lighting conditions was weaker under the higher solar irradiance in the HDI than in the LDI set-up. The HDI also yielded a decrease in the quantum yield of the SABs under all ornamental lighting conditions. Finally, the vitality of the SABs was reduced after exposure to amber + green light in the HDI set-up.

The biostatic capacity of amber + green light was validated in both LDI and HDI scenarios, which is particularly relevant in urban environments with variable solar exposure due to urban morphology or climatic factors. This research could serve to better guide

designers and/or policymakers to adapt ornamental illumination practices towards the preventive conservation of architectural heritage.

Future research should focus on proving the efficacy of the combination of amber and green LED light in terms of the effect on biodeterioration (both physical and chemical) of the substrate. Further studying the specific responses of some species like *Klebsormidium flaccidum* or whether the same principles apply to other organisms causing biodeterioration on architectural heritage, such as lichens and fungi, would also be of interest.

CRediT authorship contribution statement

Anxo Méndez: Writing – review & editing, Writing – original draft, Methodology, Investigation, Formal analysis, Conceptualization. **Rafael Carballeira:** Methodology, Investigation, Formal analysis. **Sabela Balboa:** Supervision, Methodology, Investigation, Formal analysis. **Patricia Sanmartín:** Writing – review & editing, Supervision, Project administration, Methodology, Investigation, Funding acquisition, Formal analysis.

Data accessibility

Data will be made available on request.

Declaration of competing interest

The authors declare the following financial interests/personal relationships which may be considered as potential competing interests:Anxo Mendez reports financial support was provided by Government of Galicia. Patricia Sanmartin reports financial support was provided by Government of Galicia. Sabela Balboa reports financial support was provided by Government of Galicia. Patricia Sanmartin reports financial support was provided by Spain Ministry of Science and Innovation. If there are other authors, they declare that they have no known competing financial interests or personal relationships that could have appeared to influence the work reported in this paper.

Acknowledgements

This study was conducted in the framework of the CROMALUX project: Third SMARTIAGO Challenge – Smart lighting system for Heritage Conservation. A. Méndez acknowledges the Industrial Doctorate grant (04_IN606D_2021_2598528) financed by the Xunta de Galicia. P. Sanmartín acknowledges a Ramón y Cajal contract (RYC2020-029987-I) financed by AEI/MCIU. The authors are also grateful to the Xunta de Galicia for concession of the FONTES project (ED431F 2022/14) and the Competitive Reference Group (GRC) grants ED431C 2022/09 (Gemap: A. Méndez & P. Sanmartín) and ED431C-2021/37 (Biogroup: S. Balboa).

Data availability

Data will be made available on request.

References

[1] D. Robinson, Urban morphology and indicators of radiation availability, Sol. Energy 80 (2006) 1643–1648, https://doi.org/10.1016/j.solener.2006.01.007.
[2] P. Redweik, C. Catita, M. Brito, Solar energy potential on roofs and facades in an urban landscape, Sol. Energy 97 (2013) 332–341, https://doi.org/10.1016/j.solener.2013.08.036.
[3] A. Martínez-Rubio, F. Sanz-Adan, J. Santamaría-Peña, A. Martínez, Evaluating solar irradiance over facades in high building cities, based on LiDAR technology, Appl. Energy 183 (2016) 133–147, https://doi.org/10.1016/j.apenergy.2016.08.163.
[4] R.U. Tanvir, J. Zhang, T. Canter, D. Chen, J. Lu, Z. Hu, Harnessing solar energy using phototrophic microorganisms: a sustainable pathway to bioenergy, biomaterials, and environmental solutions, Renew. Sustain. Energy Rev. 146 (2021) 111181, https://doi.org/10.1016/j.rser.2021.111181.
[5] A.A. Gorbushina, Life on the rocks, Environ. Microbiol. 9 (2007) 1613–1631, https://doi.org/10.1111/j.1462-2920.2007.01301.x.
[6] W.K. Hofbauer, G. Gärtner, Microbial Life on Façades, Springer Berlin Heidelberg, Berlin, Heidelberg, 2021, ISBN 978-3-662-54831-8.
[7] A.W. Larkum, Photosynthesis and light harvesting in algae, in: The Physiology of Microalgae, Springer International Publishing, Cham, 2016, pp. 67–87.
[8] E. Erickson, S. Wakao, K.K. Niyogi, Light stress and photoprotection in *Chlamydomonas reinhardtii*, Plant J. 82 (2015) 449–465, https://doi.org/10.1111/tpj.12825.
[9] M. DeNicola, K.D. Hoagland, Effects of solar spectral irradiance (visible to UV) on a prairie stream epilithic community, J. North Am. Benthol. Soc. 15 (1996) 155–169, https://doi.org/10.2307/1467945.
[10] A.V. Ruban, Nonphotochemical chlorophyll fluorescence quenching: mechanism and effectiveness in protecting plants from photodamage, Plant Physiol 170 (2016) 1903–1916, https://doi.org/10.1104/pp.15.01935.
[11] J.A. Raven, C.S. Cockell, Influence on photosynthesis of starlight, moonlight, planetlight, and light pollution (reflections on photosynthetically active radiation in the universe), Astrobiology 6 (2006) 668–675, https://doi.org/10.1089/ast.2006.6.668.
[12] J. Bennie, T.W. Davies, D. Cruse, K.J. Gaston, Ecological effects of artificial light at night on wild plants, J. Ecol. 104 (2016) 611–620, https://doi.org/10.1111/1365-2745.12551.
[13] C. Gardner, The use and misuse of coloured light in the urban environment, Opt Laser Technol 38 (2006) 366–376, https://doi.org/10.1016/j.optlastec.2005.06.022.
[14] Z. Amini Khoeyi, J. Seyfabadi, Z. Ramezanpour, Effect of light intensity and photoperiod on biomass and fatty acid composition of the microalgae, Chlorella vulgaris, Aquac. Int. 20 (2012) 41–49, https://doi.org/10.1007/s10499-011-9440-1.
[15] M.J. Wynne, J.K. Hallan, Reinstatement of *Tetradesmus* G. M. Smith (sphaeropleales, chlorophyta), Feddes Repert. 126 (2015) 83–86, https://doi.org/10.1002/fedr.201500021.

[16] I. Krzemińska, B. Pawlik-Skowrońska, M. Trzcińska, J. Tys, Influence of photoperiods on the growth rate and biomass productivity of green microalgae, Bioproc. Biosyst. Eng. 37 (2014) 735–741, https://doi.org/10.1007/s00449-013-1044-x.

[17] U. Karsten, S. Lembcke, R. Schumann, The effects of ultraviolet radiation on photosynthetic performance, growth and sunscreen compounds in aeroterrestrial biofilm algae isolated from building facades, Planta 225 (2007) 991–1000, https://doi.org/10.1007/s00425-006-0406-x.

[18] L. Katarzyna, G. Sai, O.A. Singh, Non-enclosure methods for non-suspended microalgae cultivation: literature review and research needs, Renew. Sustain. Energy Rev. 42 (2015) 1418–1427, https://doi.org/10.1016/j.rser.2014.11.029.

[19] Council of Europe Convention for the Protection of the Architectural Heritage of Europe 1985, 1-8.

[20] F. Rossi, E. Micheletti, L. Bruno, S.P. Adhikary, P. Albertano, R. De Philippis, Characteristics and role of the exocellular polysaccharides produced by five cyanobacteria isolated from phototrophic biofilms growing on stone monuments, Biofouling 28 (2012) 215–224, https://doi.org/10.1080/08927014.2012.663751.

[21] D. Pinna, Coping with Biological Growth on Stone Heritage Objects, Apple Academic Press: Toronto ; [Waretown, New Jersey] : Apple Academic Press, 2017. |, 2017. ISBN 9781315365510.

[22] N. Cutler, H. Viles, Eukaryotic microorganisms and stone biodeterioration, Geomicrobiol. J. 27 (2010) 630–646, https://doi.org/10.1080/01490451003702933.

[23] E. Gallego-Cartagena, H. Morillas, M. Maguregui, K. Patiño-Camelo, I. Marcaida, W. Morgado-Gamero, L.F.O. Silva, J.M. Madariaga, A comprehensive study of biofilms growing on the built heritage of a caribbean industrial city in correlation with construction materials, Int. Biodeterior. Biodegrad. 147 (2020) 104874, https://doi.org/10.1016/j.ibiod.2019.104874.

[24] D. Pinna, Microbial growth and its effects on inorganic heritage materials, in: Microorganisms in the Deterioration and Preservation of Cultural Heritage, Springer International Publishing, Cham, 2021, pp. 3–35.

[25] L.O. Björn, G.C. Papageorgiou, R.E. Blankenship, Govindjee A viewpoint: why chlorophyll a? Photosynth. Res. 99 (2009) 85–98, https://doi.org/10.1007/s11120-008-9395-x.

[26] A. Kume, T. Akitsu, K.N. Nasahara, Why is chlorophyll b only used in light-harvesting systems? J. Plant Res. 131 (2018) 961–972, https://doi.org/10.1007/s10265-018-1052-7.

[27] D.K. Saini, S. Pabbi, P. Shukla, Cyanobacterial pigments: perspectives and biotechnological approaches, Food Chem. Toxicol. 120 (2018) 616–624, https://doi.org/10.1016/j.fct.2018.08.002.

[28] M.K. Mandal, NgK. Chanu, N. Chaurasia, Cyanobacterial pigments and their fluorescence characteristics: applications in research and industry, in: Advances in Cyanobacterial Biology, Elsevier, 2020, pp. 55–72.

[29] P. Albertano, L. Bruno, S. Bellezza, New strategies for the monitoring and control of cyanobacterial films on valuable lithic faces, Plant Biosystems - An International Journal Dealing with all Aspects of Plant Biology 139 (2005) 311–322, https://doi.org/10.1080/11263500500342256.

[30] P. Albertano, L. Bruno, The importance of light in the conservation of hypogean monuments, in: Molecular Biology and Cultural Heritage, Routledge, 2017, pp. 171–178.

[31] F. Borderie, B. Alaoui-Sossé, L. Aleya, Heritage materials and biofouling mitigation through UV-C irradiation in show caves: state-of-the-art practices and future challenges, Environ. Sci. Pollut. Control Ser. 22 (2015) 4144–4172, https://doi.org/10.1007/s11356-014-4001-6.

[32] J.D. Stamford, J. Stevens, P.M. Mullineaux, T. Lawson, LED lighting: a grower's guide to light spectra, Hortscience 58 (2023) 180–196, https://doi.org/10.21273/HORTSCI16823-22.

[33] A. Kume, Importance of the green color, absorption gradient, and spectral absorption of chloroplasts for the radiative energy balance of leaves, J. Plant Res. 130 (2017) 501–514, https://doi.org/10.1007/s10265-017-0910-z.

[34] D. Zafra-Castro, Criterios Para La Planificación de La Iluminación Patrimonial Desde La Conservación: Propuesta de Alumbrado Ornamental y Vial Ambiental Del Castillo de Cardona, Universitat de Barcelona, 2020.

[35] MINCOTUR Real Decreto 1890/2008, de 14 de Noviembre, Por El Que Se Aprueba El Reglamento de Eficiencia Energética En Instalaciones de Alumbrado Exterior y Sus Instrucciones Técnicas Complementarias EA-01 a EA-07.

[36] A. Méndez, B. Prieto, J.M. Aguirre i Font, P. Sanmartín, Better, not more, lighting: policies in urban areas towards environmentally-sound illumination of historical stone buildings that also halts biological colonization, Sci. Total Environ. 906 (2024) 167560, https://doi.org/10.1016/j.scitotenv.2023.167560.

[37] A. Méndez, P. Sanmartín, S. Balboa, A. Trueba-Santiso, Environmental proteomics elucidates phototrophic biofilm responses to ornamental lighting on stone-built heritage, Microb. Ecol. 87 (2024) 147, https://doi.org/10.1007/s00248-024-02465-1.

[38] H. Ettl, G. Gärtner, Syllabus Der Boden-, Luft- Und Flechtenalgen, Springer Berlin Heidelberg, Berlin, Heidelberg, 1995. ISBN 978-3-642-39461-4.

[39] L.S. Khaybullina, L.A. Gaysina, J.R. Johansen, M. Krautová, Examination of the terrestrial algae of the great smoky mountains national park, USA, Fottea 10 (2010) 201–215, https://doi.org/10.5507/fot.2010.011.

[40] K. Fuíková, V.R. Flechtner, L.A. Lewis, Revision of the genus bracteacoccus tereg (chlorophyceae, chlorophyta) based on a phylogenetic approach, Nova Hedwigia 96 (2012) 15–59, https://doi.org/10.1127/0029-5035/2012/0067.

[41] J. Komárek, Süßwasserflora von Mitteleuropa, Bd. 19/3: Cyanoprokaryota, first ed., 2013. Heidelberg.

[42] H. Utermohl, Zur ver vollkommung der quantitativen phytoplankton-methodik, Mitteilung Internationale Vereinigung Fuer Theoretische unde Amgewandte Limnologie 9 (1958) 39.

[43] R.A. Bell, M.R. Sommerfeld, Algal biomass and primary production within a temperate zone sandstone, Am. J. Bot. 74 (1987) 294–297, https://doi.org/10.1002/j.1537-2197.1987.tb08608.x.

[44] A.R. Wellburn, The spectral determination of chlorophylls a and b, as well as total carotenoids, using various solvents with spectrophotometers of different resolution, J. Plant Physiol. 144 (1994) 307–313, https://doi.org/10.1016/S0176-1617(11)81192-2.

[45] F. Villa, B. Pitts, E. Lauchnor, F. Cappitelli, P.S. Stewart, Development of a laboratory model of a phototroph-heterotroph mixed-species biofilm at the stone/air interface, Front. Microbiol. 6 (2015), https://doi.org/10.3389/fmicb.2015.01251.

[46] P. Sanmartín, F. Villa, F. Cappitelli, S. Balboa, R. Carballeira, Characterization of a Biofilm and the Pattern Outlined by Its Growth on a Granite-Built Cloister in the Monastery of San Martiño Pinario (Santiago de Compostela , NW Spain), Int. Biodeterior. Biodegrad. 147 (2020) 104871, https://doi.org/10.1016/j.ibiod.2019.104871.

[47] Michel DuBois, K.A. Gilles, J.K. Hamilton, P.A. Rebers, Fred Smith, Colorimetric method for determination of sugars and related substances, Anal. Chem. 28 (1956) 350–356, https://doi.org/10.1021/ac60111a017.

[48] M.M. Bradford, A rapid and sensitive method for the quantitation of microgram quantities of protein utilizing the principle of protein-dye binding, Anal. Biochem. 72 (1976) 248–254, https://doi.org/10.1016/0003-2697(76)90527-3.

[49] P. Wang, G. You, J. Hou, C. Wang, Y. Xu, L. Miao, T. Feng, F. Zhang, Responses of wastewater biofilms to chronic CeO2 nanoparticles exposure: structural, physicochemical and microbial properties and potential mechanism, Water Res. 133 (2018) 208–217, https://doi.org/10.1016/j.watres.2018.01.031.

[50] S. Wahidin, A. Idris, S.R.M. Shaleh, The influence of light intensity and photoperiod on the growth and lipid content of microalgae Nannochloropsis sp, Bioresour. Technol. 129 (2013) 7–11, https://doi.org/10.1016/j.biortech.2012.11.032.

[51] X. Zhang, H. Yuan, L. Guan, X. Wang, Y. Wang, Z. Jiang, L. Cao, X. Zhang, Influence of photoperiods on microalgae biofilm: photosynthetic performance, biomass yield, and cellular composition, Energies 12 (2019) 3724, https://doi.org/10.3390/en12193724.

[52] M. Mutschlechner, H. Schöbel, Illuminating life sciences: a biophysical guide to the use of chromatic and white light sources in photobiology, Photonics 11 (2024) 487, https://doi.org/10.3390/photonics11060487.

[53] C. Shu, C. Tsai, W. Liao, K. Chen, H. Huang, Effects of light quality on the accumulation of oil in a mixed culture of *Chlorella* sp. and *Saccharomyces cerevisiae*, Journal of Chemical Technology & Biotechnology 87 (2012) 601–607, https://doi.org/10.1002/jctb.2750.

[54] J. Park, J. Seo, E.E. Kwon, Microalgae production using wastewater: effect of light-emitting diode wavelength on microalgal growth, Environ. Eng. Sci. 29 (2012) 995–1001, https://doi.org/10.1089/ees.2012.0082.

[55] A. Khalili, G.D. Najafpour, G. Amini, F. Samkhaniyani, Influence of nutrients and LED light intensities on biomass production of microalgae Chlorella vulgaris, Biotechnol. Bioproc. Eng. 20 (2015) 284–290, https://doi.org/10.1007/s12257-013-0845-8.

[56] P. Kondzior, D. Tyniecki, A. Butarewicz, Influence of Color Temperature of White LED Diodes and Illumination Intensity on the Content of Photosynthetic Pigments in Chlorella Vulgaris Algae Cells. In Proceedings of the Innovations-Sustainability-Modernity-Openness Conference (ISMO'19); MDPI: Basel Switzerland, July 18 2019, 46.

[57] H. Barberousse, R.J. Lombardo, G. Tell, A. Couté, Factors involved in the colonisation of building façades by algae and cyanobacteria in France, Biofouling 22 (2006) 69–77, https://doi.org/10.1080/08927010600564712.

[58] M. Ramírez, M. Hernández-Mariné, E. Novelo, M. Roldán, Cyanobacteria-containing biofilms from a mayan monument in palenque, Mexico, Biofouling 26 (2010) 399–409, https://doi.org/10.1080/08927011003660404.

[59] O. Guillitte, R. Dreesen, Laboratory chamber studies and petrographical analysis as bioreceptivity assessment tools of building materials, Sci. Total Environ. 167 (1995) 365–374, https://doi.org/10.1016/0048-9697(95)04596-S.

[60] A. Rifón-Lastra, Á. Noguerol-Seoane, Green algae associated with the granite walls of monuments in Galicia (NW Spain), Cryptogam. Algol. 22 (2001) 305–326, https://doi.org/10.1016/S0181-1568(01)01069-8.

[61] E. Fuentes, R. Carballeira, B. Prieto, Role of exposure on the microbial consortiums on historical rural granite buildings, Applied Sciences 11 (2021) 3786, https://doi.org/10.3390/app11093786.

[62] S. Eyssautier-Chuine, N. Vaillant-Gaveau, M. Gommeaux, C. Thomachot-Schneider, J. Pleck, G. Fronteau, Efficacy of different chemical mixtures against green algal growth on limestone: a case study with Chlorella vulgaris, Int. Biodeterior. Biodegrad. 103 (2015) 59–68, https://doi.org/10.1016/j.ibiod.2015.02.021.

[63] A. Hindáková, F. Hindák, Green algae of five city fountains in Bratislava, Biologia-Bratislava 53 (1998) 481–494.

[64] W. De Muynck, A.M. Ramirez, N. De Belie, W. Verstraete, Evaluation of strategies to prevent algal fouling on white architectural and cellular concrete, Int. Biodeterior. Biodegrad. 63 (2009) 679–689, https://doi.org/10.1016/j.ibiod.2009.04.007.

[65] S. Manso, W. De Muynck, I. Segura, A. Aguado, K. Steppe, N. Boon, N. De Belie, Bioreceptivity evaluation of cementitious materials designed to stimulate biological growth, Sci. Total Environ. 481 (2014) 232–241, https://doi.org/10.1016/j.scitotenv.2014.02.059.

[66] L. Tomaselli, G. Lamenti, M. Bosco, P. Tiano, Biodiversity of photosynthetic micro-organisms dwelling on stone monuments, Int. Biodeterior. Biodegrad. 46 (2000) 251–258, https://doi.org/10.1016/S0964-8305(00)00078-0.

[67] D. Vázquez-Nion, J. Rodríguez-Castro, M.C. López-Rodríguez, I. Fernández-Silva, B. Prieto, Subaerial biofilms on granitic historic buildings: microbial diversity and development of phototrophic multi-species cultures, Biofouling 32 (2016) 657–669, https://doi.org/10.1080/08927014.2016.1183121.

[68] B. Pereira de Oliveira, A. Miller, M.A. Sequeira Braga, M.F. Macedo, A. Dionisio, T. Silveira, Characterization of Dark Films in Granites. The Case Study of Igreja Da Ordem de Sao Francisco in Oporto (Portugal), in: C. Urzì (Ed.), Proceedings of the Proceedings of the 14th Interational Biodeterioration and Biodegradation Symposium, International Biodeterioration and Biodegradation Society, 2008, p. 72. Messina.

[69] M.F. Macedo, A.Z. Miller, A. Dionísio, C. Saiz-Jimenez, Biodiversity of cyanobacteria and green algae on monuments in the mediterranean basin: an overview, Microbiology (N. Y.) 155 (2009) 3476–3490, https://doi.org/10.1099/mic.0.032508-0.

[70] C.C. Gaylarde, P.M. Gaylarde, A comparative study of the major microbial biomass of biofilms on exteriors of buildings in europe and Latin America, Int. Biodeterior. Biodegrad. 55 (2005) 131–139, https://doi.org/10.1016/j.ibiod.2004.10.001.

[71] A.M. Bellinzoni, G. Caneva, S. Ricci, Ecological trends in travertine colonisation by pioneer algae and plant communities, Int. Biodeterior. Biodegrad. 51 (2003) 203–210, https://doi.org/10.1016/S0964-8305(02)00172-5.

[72] C.A. Crispim, P.M. Gaylarde, C.C. Gaylarde, Algal and cyanobacterial biofilms on calcareous historic buildings, Curr. Microbiol. 46 (2003) 79–82, https://doi.org/10.1007/s00284-002-3815-5.

[73] M.N. Metsoviti, G. Papapolymerou, I.T. Karapanagiotidis, N. Katsoulas, Effect of light intensity and quality on growth rate and composition of Chlorella vulgaris, Plants 9 (2019) 31, https://doi.org/10.3390/plants9010031.

[74] U. Karsten, A. Holzinger, Green algae in alpine biological soil crust communities: acclimation strategies against ultraviolet radiation and dehydration, Biodivers. Conserv. 23 (2014) 1845–1858, https://doi.org/10.1007/s10531-014-0653-2.

[75] S. Sharma, A.K. Gautam, R. Singh, S. Gourinath, S. Kateriya, Unusual photodynamic characteristics of the light-oxygen-voltage domain of phototropin linked to terrestrial adaptation of *Klebsormidium nitens*, FEBS J. (2024), https://doi.org/10.1111/febs.17284.

[76] F.-W. Li, C.J. Rothfels, M. Melkonian, J.C. Villarreal, D.W. Stevenson, S.W. Graham, G.K.-S. Wong, S. Mathews, K.M. Pryer, The origin and evolution of phototropins, Front. Plant Sci. 6 (2015), https://doi.org/10.3389/fpls.2015.00637.

[77] M. Komar, P. Nowicka-Krawczyk, T. Ruman, J. Nizioł, M. Dudek, B. Gutarowska, Biodeterioration potential of algae on building materials - model study, Int. Biodeterior. Biodegrad. 180 (2023) 105593, https://doi.org/10.1016/j.ibiod.2023.105593.

[78] A. Negi, I.P. Sarethy, Microbial biodeterioration of cultural heritage: events, colonization, and analyses, Microb. Ecol. 78 (2019) 1014–1029, https://doi.org/10.1007/s00248-019-01366-y.

[79] J.-Y. Lee, S.-H. Seo, C.-Y. Ahn, C.S. Lee, K.-G. An, A. Srivastava, H.-M. Oh, Green light as supplementary light for enhancing biomass production of Ettlia sp. and preventing population invasion from other microalgae, J. Appl. Phycol. 31 (2019) 2207–2215, https://doi.org/10.1007/s10811-019-1737-x.

[80] K. Chekanov, Diversity and distribution of carotenogenic algae in europe: a review, Mar. Drugs 21 (2023) 108, https://doi.org/10.3390/md21020108.

[81] A. Méndez, F. Maisto, J. Pavlović, M. Rusková, D. Pangallo, P. Sanmartín, Microbiome shifts elicited by ornamental lighting of granite facades identified by MinION sequencing, J. Photochem. Photobiol., B 261 (2024) 113065, https://doi.org/10.1016/j.jphotobiol.2024.113065.

[82] Y. Bao, Y. Ma, W. Liu, X. Li, Y. Li, P. Zhou, Y. Feng, M. Delgado-Baquerizo, Innovative strategy for the conservation of a millennial mausoleum from biodeterioration through artificial light management, NPJ Biofilms Microbiomes 9 (2023) 69, https://doi.org/10.1038/s41522-023-00438-9.

[83] S. Popović, M. Pećić, G. Subakov Simić, Exploring Lampenflora of Resavska Cave, Serbia. In Proceedings of the the 2nd International Electronic Conference on Diversity (IECD 2022)—New Insights into the Biodiversity of Plants, Animals and Microbes; MDPI: Basel Switzerland, March 15 2022, 33.

[84] V.M. Luimstra, J.M. Schuurmans, K.J. Hellingwerf, H.C.P. Matthijs, J. Huisman, Blue light induces major changes in the gene expression profile of the cyanobacterium <scp> *Synechocystis* </Scp> sp. PCC 6803, Physiol Plant 170 (2020) 10–26, https://doi.org/10.1111/ppl.13086.

[85] H. Matsui, K. Anraku, T. Kotani, Spectrophotometry can monitor changes in algal metabolism triggered by nutrient deficiency in Nannochloropsis oculata cultured under various light-emitting diode light regimes, Fisheries Science 85 (2019) 167–176, https://doi.org/10.1007/s12562-018-1261-y.

[86] P. Dahech, M. Schlömann, C. Ortiz, Light intensity stimulates the production of extracellular polymeric substances (EPS) in a culture of the desert cyanobacterium trichormus sp, J. Appl. Phycol. 33 (2021) 2795–2804, https://doi.org/10.1007/s10811-021-02516-x.

[87] H. Ge, J. Zhang, X. Zhou, L. Xia, C. Hu, Effects of light intensity on components and topographical structures of extracellular polymeric substances from *Microcoleus vaginatus* (cyanophyceae), Phycologia 53 (2014) 167–173, https://doi.org/10.2216/13-163.1.

[88] D. Kumar, J. Kvíderová, P. Kaštánek, J. Lukavský, The green alga *Dictyosphaerium chlorelloides* biomass and polysaccharides production determined using cultivation in crossed gradients of temperature and light, Eng. Life Sci. 17 (2017) 1030–1038, https://doi.org/10.1002/elsc.201700014.

[89] J.P. Pavissich, M. Li, R. Nerenberg, Spatial distribution of mechanical properties in *Pseudomonas aeruginosa* biofilms, and their potential impacts on biofilm deformation, Biotechnol. Bioeng. 118 (2021) 1545–1556, https://doi.org/10.1002/bit.27671.

[90] W. Liu, Y. Ji, Y. Long, W. Huang, C. Zhang, H. Wang, Y. Xu, Z. Lei, W. Huang, D. Liu, The role of light wavelengths in regulating algal-bacterial granules formation, protein and lipid accumulation, and microbial functions, J Environ Manage 337 (2023) 117750, https://doi.org/10.1016/J.JENVMAN.2023.117750.

[91] Y. Shen, H. Zhang, X. Xu, X. Lin, Biofilm Formation and lipid accumulation of attached culture of Botryococcus braunii, Bioproc. Biosyst. Eng. 38 (2015) 481–488, https://doi.org/10.1007/s00449-014-1287-1.

[92] V. Urbain, J.C. Block, J. Manem, Bioflocculation in activated sludge: an analytic approach, Water Res. 27 (1993) 829–838, https://doi.org/10.1016/0043-1354(93)90147-A.

[93] Y.T. Cheah, D.J.C. Chan, Physiology of microalgal biofilm: a review on prediction of adhesion on substrates, Bioengineered 12 (2021) 7577–7599, https://doi.org/10.1080/21655979.2021.1980671.

[94] H.T. Schroeder, C.H. De Lemos Muller, T.G. Heck, M. Krause, P.I. Homem de Bittencourt, The dance of proteostasis and metabolism: unveiling the caloristatic controlling switch, Cell Stress Chaperones 29 (2024) 175–200, https://doi.org/10.1016/j.cstres.2024.02.002.
[95] C. Honeywill, D. Paterson, S. Hagerthey, Determination of microphytobenthic biomass using pulse-amplitude modulated minimum fluorescence, Eur. J. Phycol. 37 (2002) 485–492, https://doi.org/10.1017/S0967026202003888.
[96] W. Stock, L. Blommaert, I. Daveloose, W. Vyverman, K. Sabbe, Assessing the suitability of imaging-PAM fluorometry for monitoring growth of benthic diatoms, J. Exp. Mar. Biol. Ecol. 513 (2019) 35–41, https://doi.org/10.1016/J.JEMBE.2019.02.003.
[97] A. Eggert, N. Häubner, S. Klausch, U. Karsten, R. Schumann, Quantification of algal biofilms colonising building materials: chlorophyll α measured by PAM-fluorometry as a biomass parameter, Biofouling 22 (2006) 79–90, https://doi.org/10.1080/08927010600579090.
[98] M. Michel-Rodriguez, S. Lefebvre, M. Crouvoisier, X. Mériaux, F. Lizon, Underwater light climate and wavelength dependence of microalgae photosynthetic parameters in a temperate sea, PeerJ 9 (2021) e12101, https://doi.org/10.7717/peerj.12101.
[99] I. Terashima, T. Fujita, T. Inoue, W.S. Chow, R. Oguchi, Green light drives leaf photosynthesis more efficiently than red light in strong white light: revisiting the enigmatic question of why leaves are green, Plant Cell Physiol. 50 (2009) 684–697, https://doi.org/10.1093/pcp/pcp034.
[100] W. Blanken, M. Cuaresma, R.H. Wijffels, M. Janssen, Cultivation of microalgae on artificial light comes at a cost, Algal Res. 2 (2013) 333–340, https://doi.org/10.1016/j.algal.2013.09.004.
[101] I. Terashima, T. Fujita, T. Inoue, W.S. Chow, R. Oguchi, Green light drives leaf photosynthesis more efficiently than red light in strong white light: revisiting the enigmatic question of why leaves are green, Plant Cell Physiol. 50 (2009) 684–697, https://doi.org/10.1093/PCP/PCP034.
[102] J. Chauhan, M.D. Prathibha, P. Singh, P. Choyal, U.N. Mishra, D. Saha, R. Kumar, H. Anuragi, S. Pandey, B. Bose, et al., Plant photosynthesis under abiotic stresses: damages, adaptive, and signaling mechanisms, Plant Stress 10 (2023) 100296, https://doi.org/10.1016/J.STRESS.2023.100296.
[103] Y. Wang, T. Qu, X. Zhao, X. Tang, H. Xiao, X. Tang, A comparative study of the photosynthetic capacity in two green tide macroalgae using chlorophyll fluorescence, SpringerPlus 5 (2016) 775, https://doi.org/10.1186/s40064-016-2488-7.
[104] F.L. Figueroa, R. Conde-Álvarez, I. Gómez, Relations between electron transport rates determined by pulse amplitude modulated chlorophyll fluorescence and oxygen evolution in macroalgae under different light conditions, Photosynth. Res. 75 (2003) 259–275, https://doi.org/10.1023/A:1023936313544.
[105] P. Juneau, B.R. Green, P.J. Harrison, Simulation of pulse-amplitude-modulated (PAM) fluorescence: limitations of some PAM-parameters in studying environmental stress effects, Photosynthetica 43 (2005) 75–83, https://doi.org/10.1007/S11099-005-5083-7/METRICS.
[106] A. Meneghesso, Investigation of mechanisms modulating photosynthetic efficiency in Nannochloropsis gaditana. Università degli Studi di Padova: Padova, 2016.
[107] K. Roháček, Chlorophyll fluorescence parameters: the definitions, photosynthetic meaning, and mutual relationships, Photosynthetica 40 (2002) 13–29, https://doi.org/10.1023/A:1020125719386/METRICS.
[108] I. Rodea-Palomares, S. Gonzalo, J. Santiago-Morales, F. Leganés, E. García-Calvo, R. Rosal, F. Fernández-Piñas, An insight into the mechanisms of nanoceria toxicity in aquatic photosynthetic organisms, Aquat. Toxicol. 122–123 (2012) 133–143, https://doi.org/10.1016/j.aquatox.2012.06.005.